

Ligand-Based Design of Allosteric Retinoic Acid Receptor-Related Orphan Receptor #t (ROR#t) Inverse Agonists

Femke Meijer, Richard G. Doveston, Rens de Vries, Gael Vos, Alex Vos, Seppe Leysen, Marcel Scheepstra, Christian Ottmann, Lech-Gustav Milroy, and Luc Brunsveld

J. Med. Chem., **Just Accepted Manuscript** • DOI: 10.1021/acs.jmedchem.9b01372 • Publication Date (Web): 10 Dec 2019

Downloaded from pubs.acs.org on December 10, 2019

Just Accepted

"Just Accepted" manuscripts have been peer-reviewed and accepted for publication. They are posted online prior to technical editing, formatting for publication and author proofing. The American Chemical Society provides "Just Accepted" as a service to the research community to expedite the dissemination of scientific material as soon as possible after acceptance. "Just Accepted" manuscripts appear in full in PDF format accompanied by an HTML abstract. "Just Accepted" manuscripts have been fully peer reviewed, but should not be considered the official version of record. They are citable by the Digital Object Identifier (DOI®). "Just Accepted" is an optional service offered to authors. Therefore, the "Just Accepted" Web site may not include all articles that will be published in the journal. After a manuscript is technically edited and formatted, it will be removed from the "Just Accepted" Web site and published as an ASAP article. Note that technical editing may introduce minor changes to the manuscript text and/or graphics which could affect content, and all legal disclaimers and ethical guidelines that apply to the journal pertain. ACS cannot be held responsible for errors or consequences arising from the use of information contained in these "Just Accepted" manuscripts.

Ligand-Based Design of Allosteric Retinoic Acid Receptor-Related Orphan Receptor γ t (ROR γ t) Inverse Agonists

*Femke A. Meijer,^{§,‡} Richard G. Doveston,^{§,‡,§} Rens M.J.M. de Vries,[‡] Gaël M. Vos,[‡] Alex
A.A. Vos,[‡] Seppe Leysen,[‡] Marcel Scheepstra,[‡] Christian Ottmann,[‡] Lech-Gustav Milroy,[‡]
and Luc Brunsveld^{‡,*}*

[§]These authors contributed equally to this work.

AUTHOR ADDRESS

[‡] Laboratory of Chemical Biology, Department of Biomedical Engineering and Institute
for Complex Molecular Systems, Technische Universiteit Eindhoven, Den Dolech 2,
5612 AZ Eindhoven, The Netherlands

[§] Leicester Institute of Structural and Chemical Biology and Department of Chemistry,
University of Leicester, University Road, Leicester, UK, LE1 7RH.

1
2
3
4
5
6
7
8
9
10
11
12
13
14
15
16
17
18
19
20
21
22
23
24
25
26
27
28
29
30
31
32
33
34
35
36
37
38
39
40
41
42
43
44
45
46
47
48
49
50
51
52
53
54
55
56
57
58
59
60

KEYWORDS

Nuclear Receptors • ROR γ t • Allosteric Modulators • Ligand-Based Design • Drug

Discovery

ABSTRACT

Retinoic acid receptor-related orphan receptor γ (ROR γ) is a nuclear receptor associated with the pathogenesis of autoimmune diseases. Allosteric inhibition of ROR γ is conceptually new, unique for this specific nuclear receptor, and offers advantages over traditional orthosteric inhibition. Here, we report a highly efficient *in silico*-guided approach that led to the discovery of novel allosteric ROR γ inverse agonists with a distinct isoxazole chemotype. The most potent compound, **25**, displayed sub-micromolar inhibition in a coactivator recruitment assay and effectively reduced IL-17a mRNA production in EL4 cells, a marker of ROR γ activity. The projected allosteric mode of action of **25** was confirmed by biochemical experiments and co-crystallization with the ROR γ ligand binding domain. The isoxazole compounds have promising pharmacokinetic properties comparable to other allosteric ligands, but with a more diverse chemotype. The efficient ligand-based design approach adopted demonstrates its versatility in generating chemical diversity for allosteric targeting of ROR γ .

1. INTRODUCTION

The nuclear receptor (NR) ROR γ t has emerged as an important therapeutic target in recent years because of its important role in both cancer and autoimmune disease. Inhibition of ROR γ t is a promising therapeutic strategy for the treatment of prostate cancer because it stimulates androgen receptor (AR) gene transcription.^{1,2} However, ROR γ t is most prominently targeted for inhibition because of its essential role in promoting T helper 17 (Th17) cell differentiation.³⁻⁵ Th17 cells produce the cytokine IL-17 which is strongly implicated in the pathogenesis of autoimmune diseases⁶ such as psoriasis,⁷ multiple sclerosis⁸ and inflammatory bowel disease.⁹ Disrupting the Th17/IL-17 pathway using IL-17 monoclonal antibodies (mAb) is a successful therapeutic strategy, with three mAbs approved for the treatment of plaque psoriasis: secukinumab (Cosentyx),¹⁰ brodalumab (Siliq),¹¹ and ixekizumab (Taltz).¹² Inhibition of ROR γ t with small molecules to disrupt the Th17/IL-17 pathway has been the focus of much research in recent years,¹³⁻²⁰ with several compounds progressed to clinical trials.²

ROR γ t contains a hydrophobic ligand binding pocket located within a ligand binding domain (LBD) that is highly conserved across the NR family.²¹ However, its transcriptional activity is not dependent on ligand binding because the apo protein retains the C-terminal helix 12 (H12) in a conformational state that allows for partial recruitment of coactivator proteins.^{22,23} Although formally an orphan receptor with no proven endogenous ligands, ROR γ t is responsive to binding of naturally occurring cholesterol derivatives. Hydroxycholesterols have been shown to be effective agonists that stabilize H12 in such a way to further promote coactivator binding.²⁴ In contrast, digoxin (**1**, Figure 1) is an inverse agonist that stabilizes H12 in a conformation that is unsuitable for coactivator binding but promotes corepressor binding, thus leading to diminished

gene transcription.²⁵ Numerous synthetic inverse agonists are also known, including T0901317 (**2**, Figure 1).²⁶ In all these cases, the ligands target the same orthosteric ligand binding pocket (Figure 1).

NR orthosteric ligand binding pockets are the target for numerous and highly effective drug molecules.²⁷ Nevertheless, the highly conserved nature of this pocket across the NR family has led to issues associated with selectivity and mutation-induced resistance. Furthermore, dosing levels must be appropriate to compete with endogenous ligands. Molecules that target allosteric binding sites on NRs could circumvent such problems, for example because of the chemical uniqueness of the pocket and the absence of a competitive endogenous ligand. Such allosteric compounds are therefore extremely valuable for both drug discovery and chemical biology applications.²⁸⁻³⁰ The discovery that the potent ROR γ t inverse agonists MRL-871 (**3**, Figure 1)³¹ and later **4**³² target a previously unreported allosteric binding site within the ROR γ t LBD was therefore highly significant. These ligands were observed to directly interact with the activation function loop between H11 and H12 (AF-2 domain), thus forcing H12 to adopt an unusual conformation that prevents coactivator recruitment (Figure 1).³¹

Orthosteric Inverse Agonists

Allosteric Inverse Agonists

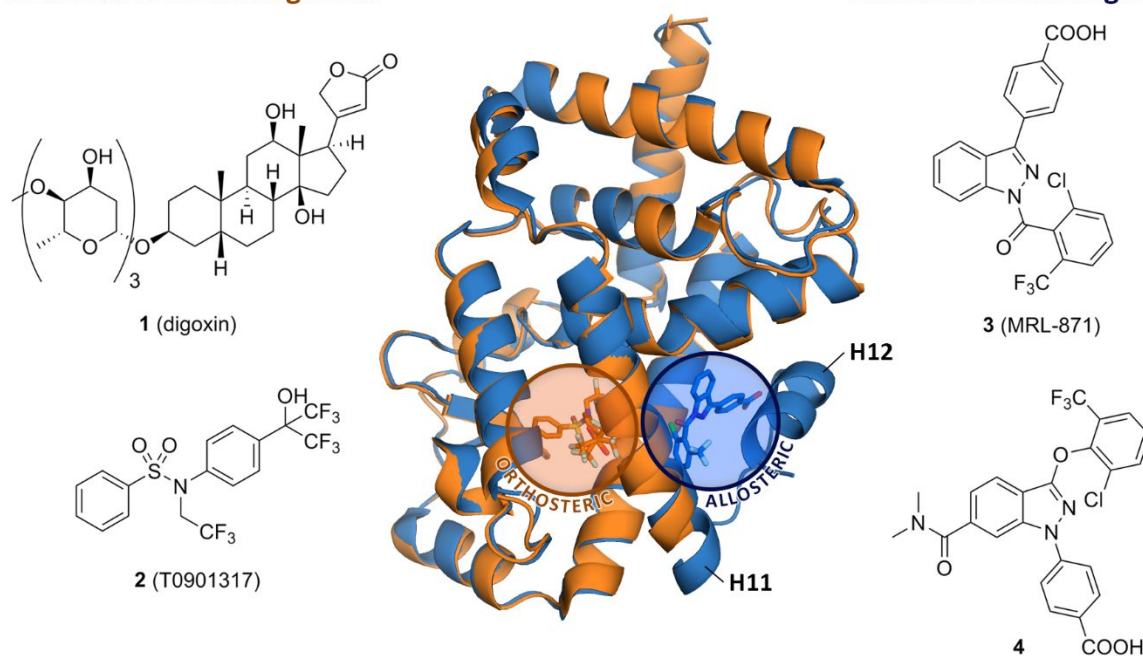


Figure 1. Orthosteric and allosteric ROR γ t ligand binding sites are shown by overlay of the crystal structures of ROR γ t LBD in complex with orthosteric inverse agonist **2** (orange, PDB code: 4NB6) and allosteric inverse agonist **3** (blue, PDB code: 4YPQ). The structures of the orthosteric inverse agonist **1** and allosteric inverse agonist **4** are also shown.

Allosteric modulation of ROR γ t has enormous potential as a novel therapeutic strategy; but, the examples of ligands that unambiguously target the allosteric pocket have been limited to compounds based on closely related chemotypes containing indazole or imidazopyridine cores.²⁸ As an example, indazoles **3** and **4** displayed promising *in vivo* activity,^{33,34} but challenges remain, such as PPAR γ cross-activity and pharmacokinetic (PK) profiles, for which novel chemotypes are

needed.¹⁵ In order to better exploit the strategy of allosteric modulation for therapeutic purposes, there is thus an urgent need to identify novel chemotypes targeting the allosteric site. In this study, we report the design, synthesis and evaluation of a novel class of ROR γ t allosteric inverse agonists. The novel chemotype, discovered by *in silico*-guided pharmacophore screening and optimization, is based on a trisubstituted isoxazole core that, following efficient optimization of two substituents, led to the discovery of a sub-micromolar inverse agonist. Protein X-ray crystallography and biophysical data unambiguously proved the designed allosteric mode of action. The compounds effectively inhibit cellular IL-17a expression and thus constitute valuable leads in the development of treatments for autoimmune diseases. To the best of our knowledge, our highly efficient *in silico*-guided approach is the first example of a medicinal chemistry program to overtly identify and develop a novel chemotype that targets the ROR γ t allosteric site.

2. RESULTS AND DISCUSSION

2.1. *In Silico* Pharmacophore Screen

In order to identify novel chemotypes for chemical optimization, we used the crystal structure of ROR γ t LBD in complex with **3** as the basis for an *in silico* 3D pharmacophore screen against virtual compound libraries. An analogous scaffold hopping approach had been used previously to identify similar scaffolds to **3** such as the potent inverse agonist thienopyrrazole **5** (Figure 2), although an allosteric mode of action was not proven.³⁵ We created a 3D pharmacophore hypothesis based on the crystal structure of **3** bound to the allosteric pocket using Phase (Schrödinger 2017-2).^{36,37} Six structural features of **3** known to be important for activity were incorporated in the hypothesis: the three six-membered aromatic rings, an anionic group and two hydrophobic substituents (Figure 2). This hypothesis was used to interrogate a virtual library of

289,174 compounds from the Asinex Gold-Platinum collection of drug-like molecules.³⁸ Compounds matching at least four out of the six pharmacophore features were deemed to be a good hit. These were ranked using the 'Phase Screen Score' with higher scores indicating a better alignment with the hypothesis. The Phase Screen scores for **3** and **5** were used as contextual references. The four highest ranking hit structures were all found to be based around the same trisubstituted isoxazole scaffold with **6** returned as the best match (Figure 2). This same scaffold was present in 13 of the top 30 hits. However, in each case we noted that only four out of six pharmacophore features were matched. Therefore, we designed two virtual ligands, **7** and **8**, that incorporated five and six of the features respectively. As expected this led to improved Phase Screen Scores (Figure 2) and these compounds were therefore selected as initial targets for experimental investigation.

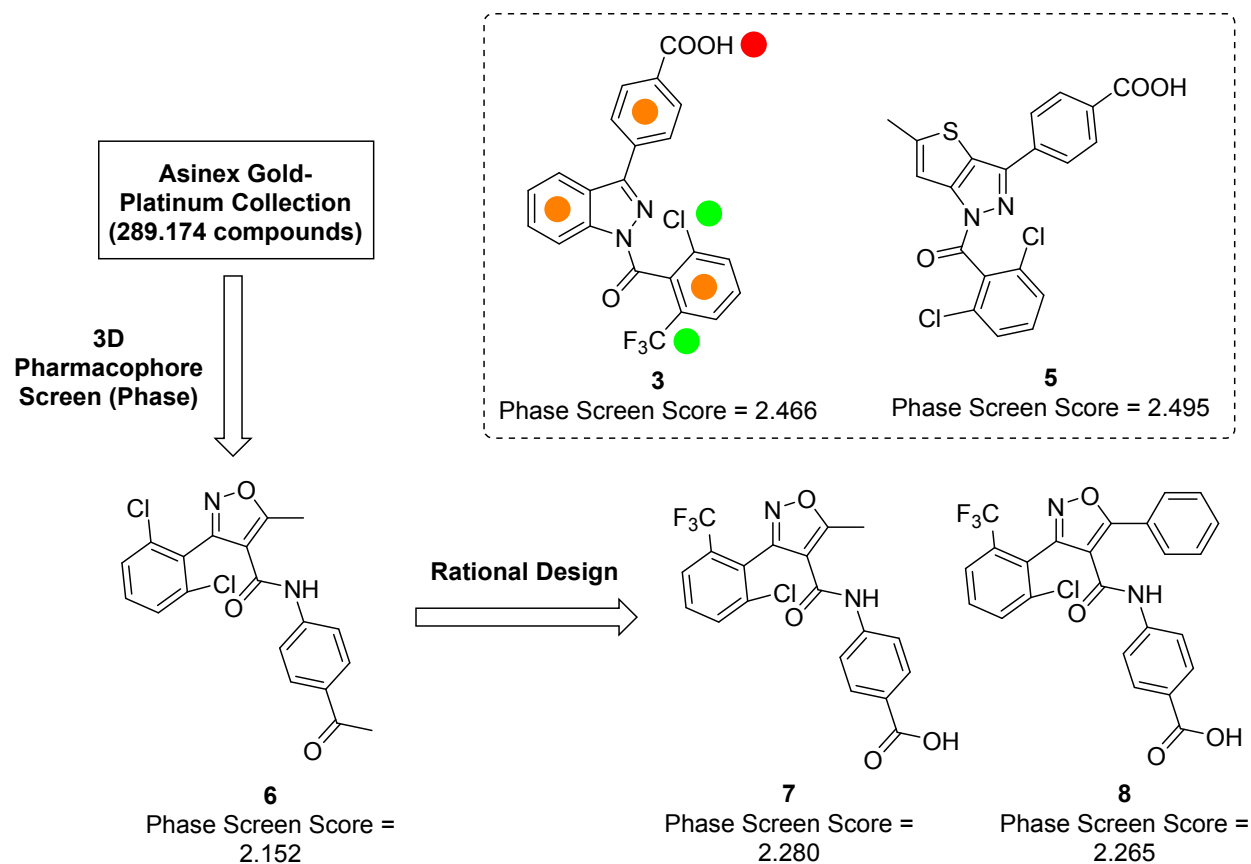
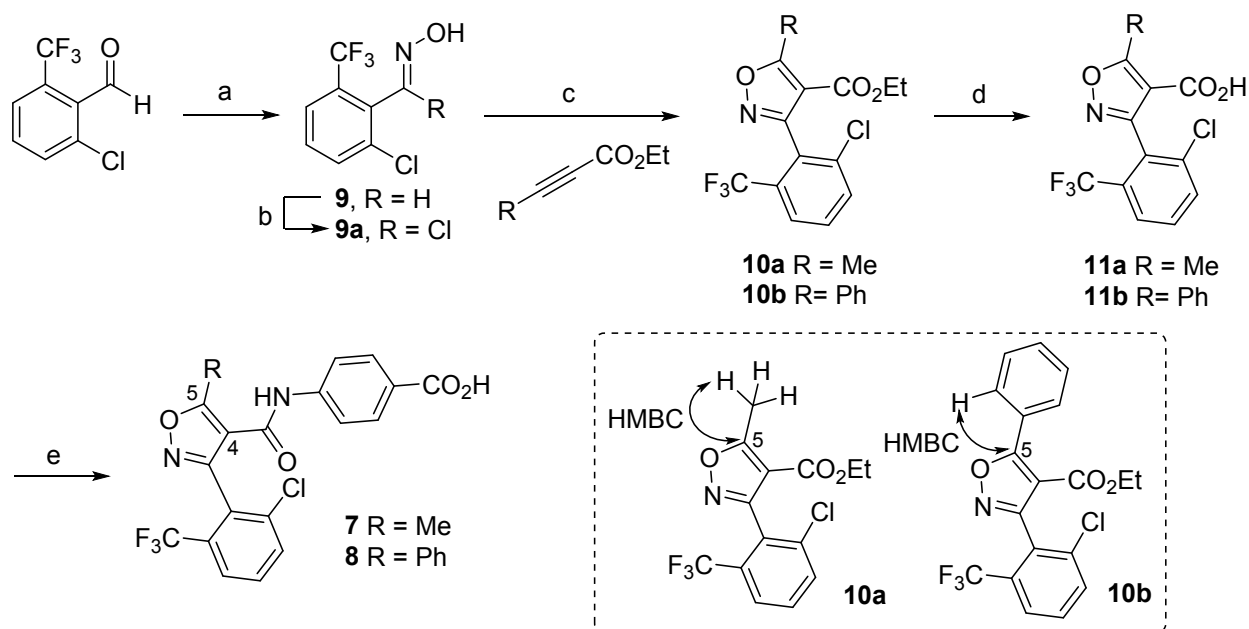


Figure 2. 3D Pharmacophore screening identifies a compound class with a novel isoxazole-based chemotype for experimental evaluation. The structural features of **3** incorporated into the pharmacophore hypothesis are indicated: orange = aromatic rings, green = hydrophobic groups, red = anionic group.

2.2. Exploratory Structure-Activity Relationship Study

Isoxazoles **7** and **8** were synthesized *via* [3+2] dipolar cycloaddition of a nitrile oxide (generated *in situ* from the oxime chloride **9a**) and a commercially available alkyne.³⁹ The regiochemistry of the resulting trisubstituted isoxazole esters **10** was confirmed by 2D-NMR experiments (key HMBC correlations are highlighted in Scheme 1). Ester hydrolysis followed by amide coupling of *tert*-butyl-4-amino benzoate via the respective acid chloride, and finally deprotection of the *tert*-butyl ester furnished the target compounds in an efficient manner (Scheme 1).

Scheme 1. Synthesis of trisubstituted isoxazoles **7** and **8**.^a Key HMBC correlations used to confirm the regiochemistry of **10a** and **10b** are shown. The ¹³C-NMR signals for the C-5 carbons are distinctively downfield at 175 and 173 ppm respectively.



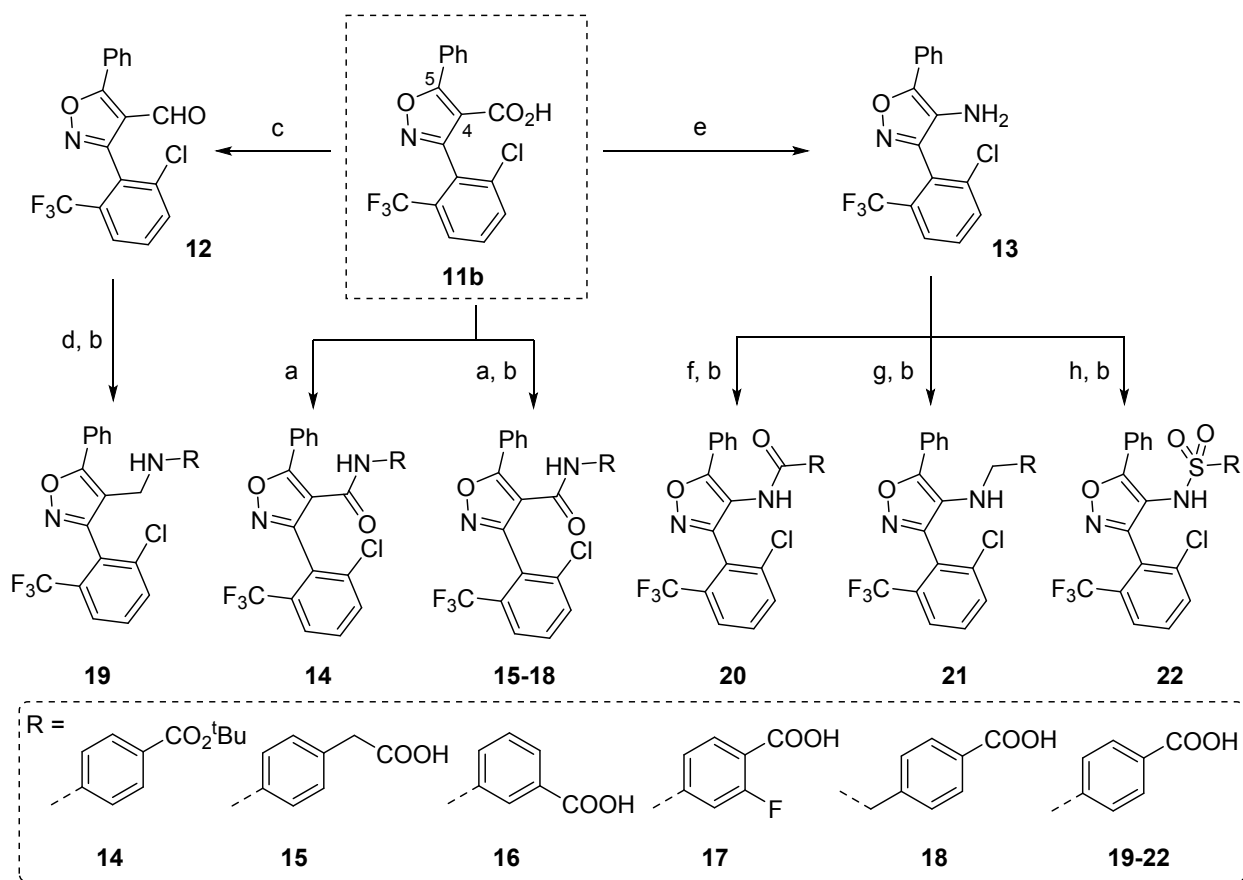
^aReagents and conditions: (a) $\text{NH}_2\text{OH}\cdot\text{HCl}$, NaOH (aq), EtOH , rt, 18 h, 83%; (b) NCS , DMF , $60\text{ }^\circ\text{C}$, 18 h, 86%; then (c) alkyne, NEt_3 , THF , $80\text{ }^\circ\text{C}$, 4 h, 69% (**10a**), 80% (**10b**); (d) LiOH , EtOH , H_2O , $70\text{ }^\circ\text{C}$, 8 h, 84% (**11a**), 95% (**11b**); (e) i) SOCl_2 , $50\text{ }^\circ\text{C}$, 2 h; ii) *tert*-butyl-4-amino benzoate, NEt_3 , CH_2Cl_2 , $45\text{ }^\circ\text{C}$, 6 h; iii) TFA , CH_2Cl_2 , rt, 18 h, 42% (**7**), 69% (**8**).

To determine if the compounds showed a functional response in terms of $\text{ROR}\gamma\text{t}$ affinity for a coactivator, **7** and **8** were tested in a time-resolved FRET (TR-FRET) coactivator recruitment assay.³¹ Remarkably, both compounds inhibited coactivator recruitment in a dose-dependent manner. The phenyl derivative **8** was found to be significantly more potent than the methyl derivative **7**: half-maximum inhibitory concentrations (IC_{50}) of $53.5 \pm 2.9\text{ }\mu\text{M}$ for **8** compared to $>100\text{ }\mu\text{M}$ for **7**. In line with previous reports, **3** and **5** were determined to be significantly more potent with an IC_{50} of $7.8 \pm 0.5\text{ nM}$ and $425 \pm 61\text{ nM}$ respectively (Table 1).

In view of these highly promising TR-FRET results with the *in silico* derived compounds around the trisubstituted isoxazole scaffold already showing activity, phenyl isoxazole **8** was selected as the focus of a subsequent structure-activity relationship (SAR) study focusing on the isoxazole C-4 position. As such, a small library of 11 derivatives was synthesized using carboxylic acid **11b** as the cornerstone intermediate (Scheme 2) and evaluated using the coactivator recruitment assay (Table 1). While limited in size, this SAR study indicated that a benzoic acid-containing

substituent at the C-4 position was essential for potency: examples bearing no C-4 substitution (**11b**), a *para*-benzoate (**14**) or a methylene carboxylic acid (**15**) showed much reduced potency compared to the initial hit. Moving the acid moiety to the *meta*-position (**16**) or adding a *meta*-fluoro substituent (**17**) somewhat lowered the activity. However, the insertion of a single methylene unit between the amide and benzoic acid moieties (**18**) led to a six-fold increase in potency compared to the initial hit. The corresponding amine (**19**) displayed similar activity. Finally, reversing the relative positions of carbonyl and nitrogen components of the amide bond (**20-22**) did not result in a corresponding increase in potency.

Scheme 2. Synthesis of C-4 isoxazole derivatives^a



^aReagents and conditions: (a) i) SOCl₂, 50 °C, 2 h; ii) NH₂R, NEt₃, CH₂Cl₂, 45 °C, 6 h, 27-87%; (b) LiOH, MeOH, H₂O, 70 °C, 8 h, 43-99%; (c) (i) SOCl₂, 50 °C, 2 h; ii) MeNH(OMe), NEt₃, CH₂Cl₂, rt, 6 h; iii) LiAlH₄, THF, 0 °C, 30 min, 65%; (d) i) Ethyl-4-aminobenzoate, AcOH, MeOH, reflux, 24 h; ii) NaCNBH₃, MeOH, reflux, 12 h, 31%; (e) i) DPPA, *t*-BuOH, 85 °C, 18 h; ii) TFA, CH₂Cl₂, rt, 8 h, 59%; (f) i) Mono-methyl terephthalate, SOCl₂, 50 °C, 2 h; ii) **13**, NEt₃, CH₂Cl₂, 76%; (g) i) Methyl-4-formyl benzoate, AcOH, MeOH, reflux, 24 h; ii) NaCNBH₃, MeOH, reflux, 18 h, 43%; (h) Methyl-4-(chlorosulfonyl)benzoate, pyridine, 60 °C, 24 h, 71%.

Table 1. Structure-Activity Relationships around the C-4 isoxazole position. TR-FRET IC₅₀ values (μM) and respective Glide docking scores are shown. TR-FRET data is recorded in triplicate; values are representative of >3 repeated experiments.

Cmpd	IC ₅₀ (μM)	Glide Score
3	0.0078 ± 0.0005	– 14.576
5	0.425 ± 0.061	– 13.109

7	> 100	– 13.372
8	53.5 ± 2.9	– 14.184
11b	> 100	– 10.130
14	> 100	n.d.
15	> 100	– 13.724
16	73.9 ± 3.4	– 12.995
17	91.1 ± 4.6	– 14.308
18	8.76 ± 0.48	– 12.020
19	9.60 ± 0.60	– 14.012
20	> 100	– 13.550
21	30.9 ± 1.3	– 13.519
22	62.6 ± 4.4	– 13.003

2.3. *In Silico* Docking Directs Secondary SAR Study

In order to further improve the potency of our compounds we next explored the SAR at the isoxazole C-5 position. For this, molecular docking (Glide, Schrodinger 2017-2)^{40,41} was used to select - with an attention to synthetic resource - C-5 substituents that were optimal for allosteric binding and therefore activity. For the study, a single C-4 substituent, the amine of compound **19** was chosen based on its experimental activity and *in silico* docking score (Table 1, *vide infra*). A virtual library of 84 C-5 analogues was enumerated using the open-source ChemT software.⁴² This library was docked against the allosteric site of ROR γ t as defined by the X-ray crystal structure of **3** in complex with the ROR γ t LBD.³¹ A single docking pose was returned for each virtual ligand and these were ranked using the 'Glide Score', an empirical measure of binding enthalpy.⁴³ We contextualized these scores by comparison to those of compounds with known activity. The results (summarized in Table 2, see supporting information for full information) indicated that smaller heteroaromatic moieties at the C-5 position would improve allosteric binding of the isoxazole ligands relative to **19** – heteroatoms at the 2-position were predicted to be optimal e.g. furan **23** and thiophene **24** (Table 2). The introduction of a hydrogen-bond donor on the ring (specifically at the 3-position) was predicted to be even more beneficial: docking poses indicated that an additional hydrogen-bonding interaction with the backbone of helix 4 might be possible (e.g. pyrrole **25**, Table 2, Figure 3). Bulkier substituents were predicted to be detrimental for binding (e.g. naphthyl **26**). To explore the predicted effect of a hydrogen-bond donating group further we interrogated a designed subset of ligands in the same docking experiment (see supporting information). None of these ligands showed an improved Glide score compared to pyrrole **25**. However, we noted that 3-hydroxyl substitution of the C-5 phenyl ring (**27**) was predicted to significantly enhance binding

relative to **19**. To validate our findings experimentally we selected a cross-section of five derivatives for synthesis (i.e. **23-27**).

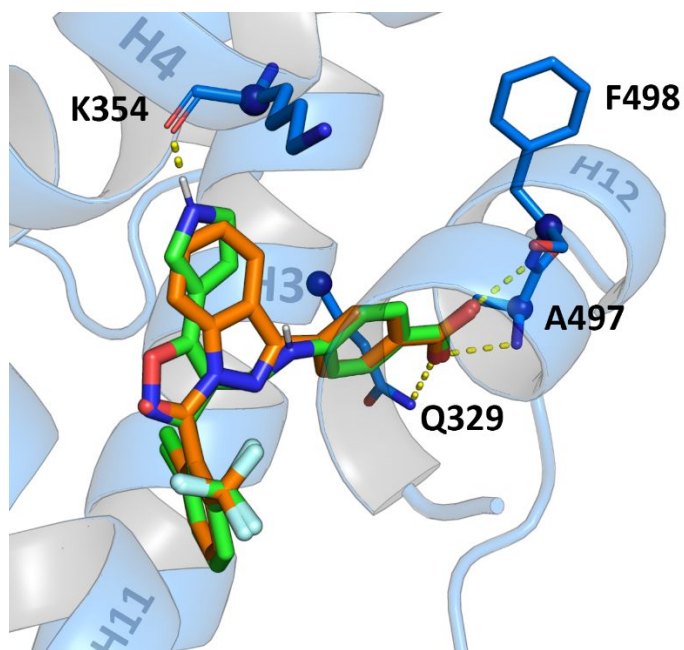
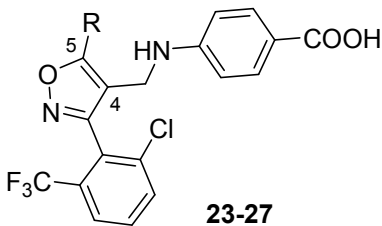


Figure 3. *In silico* modelled docking pose of **25** (green) overlaid with crystal structure of ROR γ t with **3** (orange) (PDB code: 4YPQ). For **25** the potential additional hydrogen-bond with the ROR γ t H4 backbone is indicated.

Table 2. Structure-Activity Relationships around the C-5 isoxazole position. TR-FRET IC₅₀ values (μM) and respective Glide docking scores are shown. TR-FRET data is recorded in triplicate; values are representative of >3 repeated experiments.

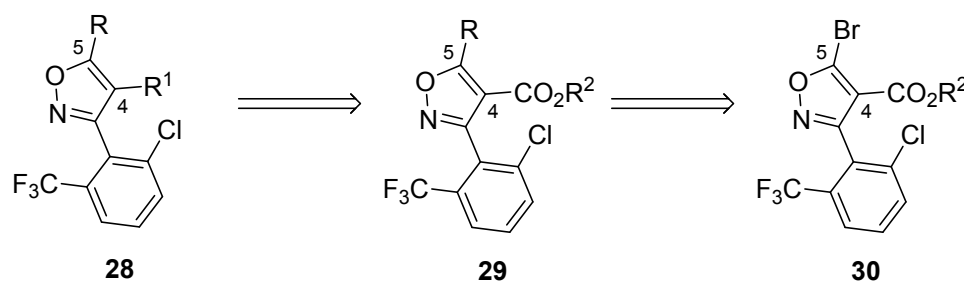


Cmpd	R	Glide Score	IC ₅₀ (μM)
19	Ph	– 14.012	9.60 ± 0.60
23		– 14.300	1.09 ± 0.09
24		– 14.182	1.75 ± 0.20
25		– 15.735	0.264 ± 0.023
26		– 10.844	> 100
27		– 14.603	6.62 ± 0.50

2.4. Docking-Guided C-5 SAR Study

To expedite the synthesis of isoxazole analogues with various C-5 and C-4 substituents we re-designed our synthetic approach. It was envisaged that 5-bromo-4-carboxy isoxazole intermediate **30** would enable later stage introduction of the desired C-5 substituents via palladium-mediated cross-coupling chemistry. Introduction of C-4 substituents by manipulation of a carbonyl functional group (as developed previously) would then be possible (Scheme 3).

Scheme 3. Retrosynthetic analysis of trisubstituted isoxazole **28** allowing for late-stage diversification.

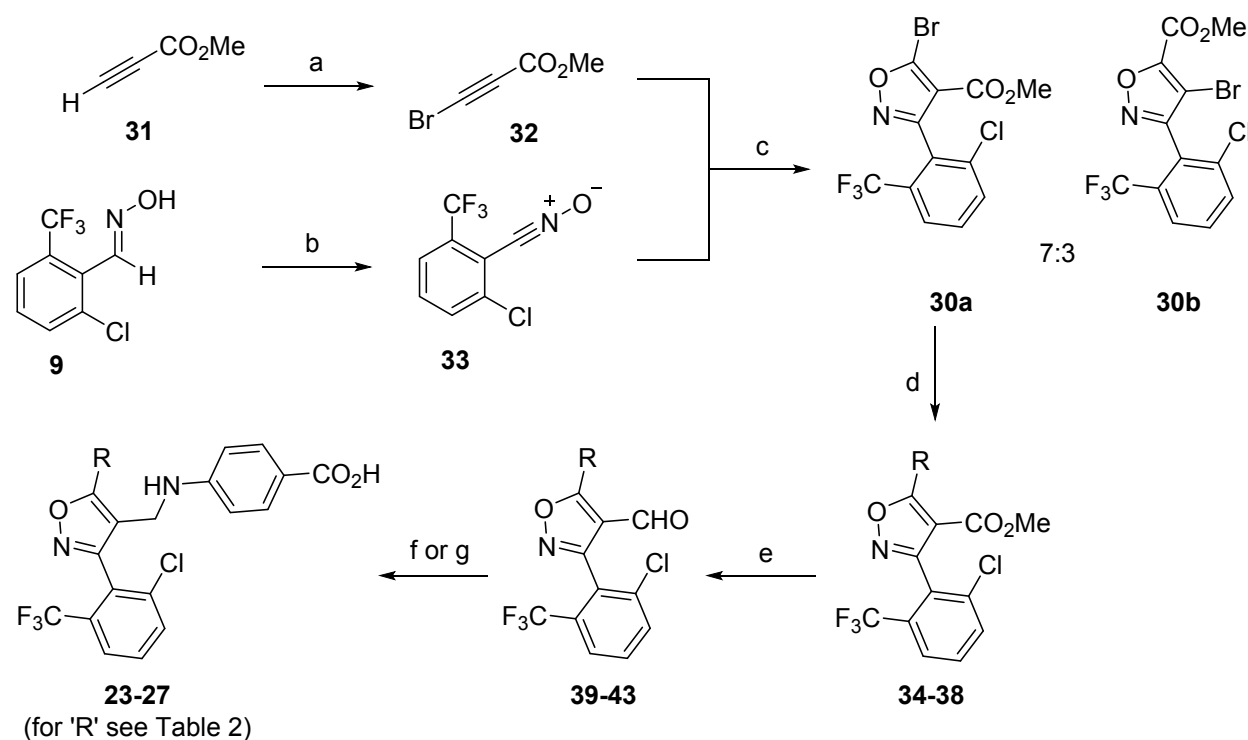


The intermediate **30** was prepared using analogous methodology to that used previously. In this case it was necessary to isolate nitrile oxide **33** prior to [3+2] cycloaddition with alkynyl bromide **32**.⁴⁴ An efficient cycloaddition reaction led to an essentially quantitative recovery of a 7:3 mixture of 5-bromoisoxazole **30a** and 4-bromoisoxazole **30b** as determined by ¹H-NMR (Scheme 4). This result was in close alignment with literature examples that indicated the 5-bromo isomer would predominate.⁴⁴ The mixture of regioisomers was purified by recrystallization from hot *n*-heptane resulting in the isolation of a 97:3 regiomer mixture (43% recovery) that was employed in subsequent steps. Assignment of the 5-bromoisoxazole **30a** as the major regioisomer was

confirmed by 2D-NMR analysis of downstream products and by synthesis via an independent route (see Supporting Information).

Scheme 4. Synthesis of isoxazole C-5 analogues **23-27**.^a 'R' groups are defined in Table

2.



^a Reagents and conditions: (a) NBS, AgNO₃, Me₂C(O), rt, 20 h, 80%; (b) i) NCS, DMF, 60 °C, 18 h, ii) NEt₃, THF, rt, 30 min, 85%; (c) THF, 80 °C, 4 h, **30a** 43%; (d) RB(pin), Pd(dppf)Cl₂, DME, 85 °C, 8 h, 39-58%; (e) i) LiAlH₄, THF, 0 °C → rt, 2 h, then ii) DMP, CH₂Cl₂, rt, 8 h, 51-96%; (f) *tert*-Butyl-4-amino benzoate, MeOH, AcOH, reflux, 24 h then ii) NaBH₄, EtOH, 85 °C, 2-6 h, 16-24%; iii) TFA, CH₂Cl₂, rt, 18 h, **23**, **24**, **26**, 48-73%; (g)

Methyl-4-amino benzoate, MeOH, AcOH, reflux, 24 h then ii) NaBH₄, MeOH, reflux, 2-4 h, 16-19%; iii) LiOH, MeOH, H₂O, 70 °C, 8 h, **25**, 57%, **27**, 99%.

The desired substituents were introduced at the C-5 position by way of a Suzuki cross-coupling with a pinacol boronate⁴⁵ (to give intermediates **34-38**) before conversion of the C-4 ester to an aldehyde (**39-43**) and reductive amination (Scheme 4). The lability of the 5-bromo group under the conditions for ester reduction dictated the order in which the synthesis steps were performed. Hydrolysis of the benzoic methyl ester to the free acid yielded the desired compounds **23-27**.

In order to explore the SAR around the isoxazole C-5 position, the five analogues prepared in this second synthesis campaign were evaluated using the HTRF coactivator recruitment assay (Table 2). We were gratified to observe that furan **23** gave a nine-fold improvement in potency compared to phenyl **19**. By comparison, thiophene **24** was slightly less potent. Most significantly, pyrrole **25**, which also showed the most beneficial Glide score, was 36-fold more potent than **19** and with an IC₅₀ value lower than the putative allosteric modulator **5**. These results were in excellent agreement with the *in silico* Glide scores obtained (Table 2) and the improvements in potency are a notable step toward emulating the high potency of indazole **3** (Figure 4-A). As predicted, the bulky naphthyl group of **26** was detrimental for activity such that no IC₅₀ curve could be fitted. The phenol derivative **27** showed a small improvement in potency compared to **19**. For this more bulky group at the C-5 position, compared to pyrrole **25**, the potential for additional hydrogen bonding, as indicated in the docking study, is thus not strongly expressed.

2.5 Mode-of-Action Studies

The allosteric mode-of-action for the novel lead compound **25** was first explored using a competitive TR-FRET coactivator recruitment assay against fixed concentrations of cholesterol (an orthosteric agonist). If an allosteric ligand and cholesterol bind in a non-competitive manner at different sites on the ROR γ t LBD then the IC₅₀ of the allosteric ligand should be independent of cholesterol concentration. By contrast, ligands competing for the same binding site should show a cholesterol-dependent activity profile whereby increasing cholesterol concentration should result in a corresponding increase in IC₅₀ of the competing ligand.³¹ In our assay, increasing concentrations of **25** perturbed coactivator recruitment in the absence of cholesterol with an IC₅₀ value of 247.8 \pm 17.7 nM. Interestingly, increasing concentrations of cholesterol indeed resulted not in an increase but in a further decrease in the IC₅₀ value for **25** with a concomitant sharpening of the Hill slope (Figure 4-B and Table 3). This result provides strong evidence not only for an allosteric mode-of-action, but also for cooperative behavior between orthosteric and allosteric ligand binding. The same profile was observed for **5** (Figure 4-C), providing the first evidence that this compound also modulates ROR γ t activity in an allosteric fashion. Indazole **3** also exhibited this behavior (Figure 4-D). By comparison, the IC₅₀ value for the orthosteric inverse agonist **1** increased as the concentration of cholesterol increased (Figure 4-E). Collectively, our competitive assay data provided strong evidence that **25** functioned as an allosteric inverse agonist.

To further confirm the allosteric mode-of-action for **25** on ROR γ t we used an orthogonal assay to directly probe for allosteric ligand binding, as opposed to measuring indirect effects on coactivator recruitment. This assay used the previously described AlexaFluor647-labelled MRL-871 derivative **44** (Figure 4-G), which upon binding to ROR γ t shows fluorescent emission as a result

1
2
3 of FRET from an anti-His terbium cryptate antibody donor.³² The results of this experiment indeed
4
5 corroborated the data obtained from the competitive cofactor recruitment assay (Figure 4-F): the
6
7 isoxazole **25** displaced the allosteric probe **44** with an $IC_{50} = 117.5 \pm 8.5$ nM, which was lower
8
9 than that of **5** ($IC_{50} = 180.0 \pm 17.5$ nM). As expected, indazole **3** was highly potent ($IC_{50} = 17.3 \pm$
10
11 1.4 nM).
12
13
14
15
16
17
18
19
20
21
22
23
24
25
26
27
28
29
30
31
32
33
34
35
36
37
38
39
40
41
42
43
44
45
46
47
48
49
50
51
52
53
54
55
56
57
58
59
60

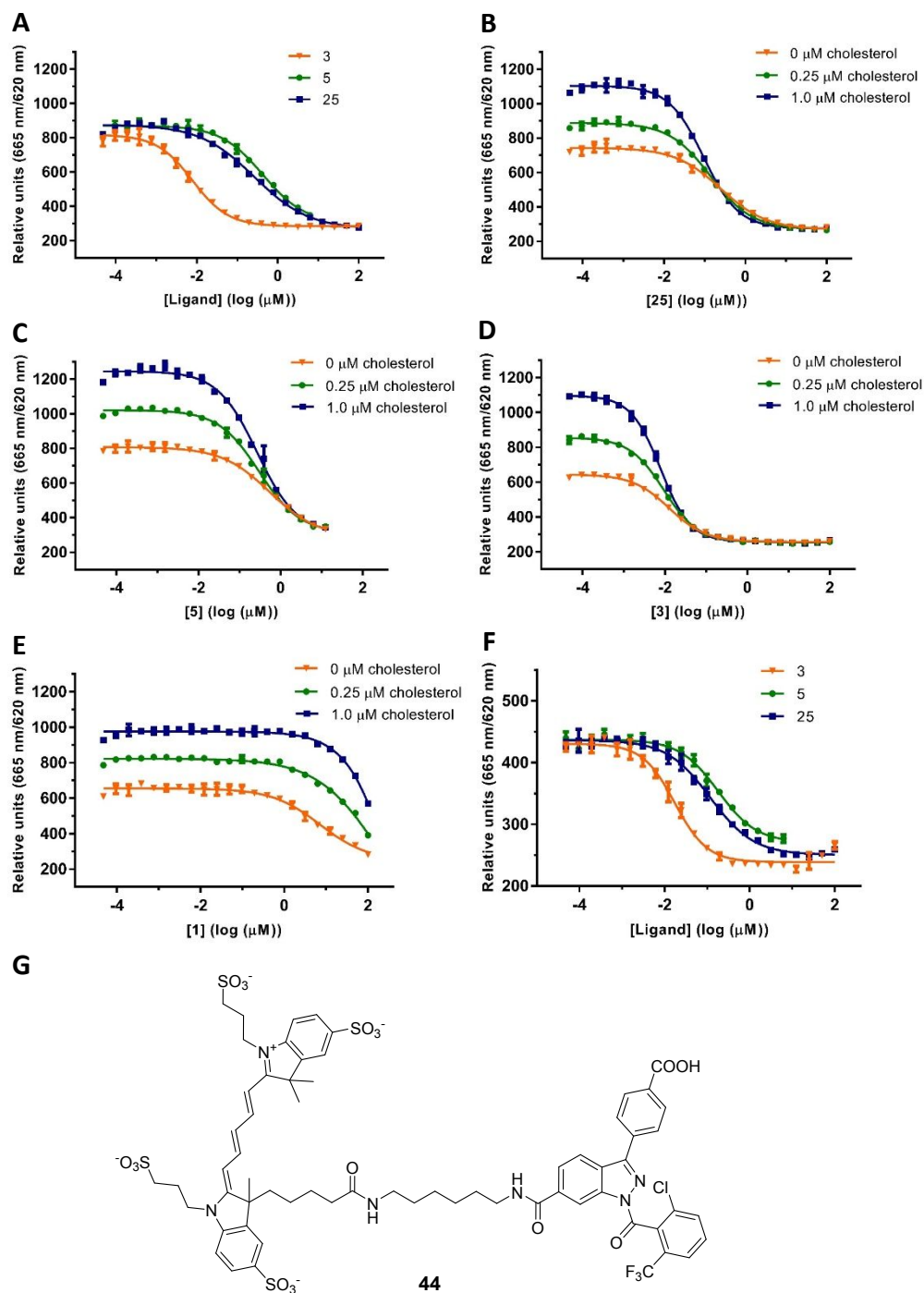


Figure 4. Biochemical ROR γ t assay data for 25, 3 and 5. (A) Dose-response curves from the TR-FRET coactivator recruitment assay; (B-E) Dose-response curves from the competitive TR-FRET coactivator recruitment assay with fixed concentrations of

cholesterol (0 μ M, 0.25 μ M and 1.0 μ M); (F) Dose-response curves from the ligand displacement HTRF assay using **44** (G) as an allosteric probe.

Table 3. IC₅₀ and Hill slope values observed in the competitive TR-FRET cofactor recruitment assay.

Compound	0 μ M Cholesterol		0.25 μ M Cholesterol		1.0 μ M Cholesterol	
	IC ₅₀ (nM)	Hill slope	IC ₅₀ (nM)	Hill slope	IC ₅₀ (nM)	Hill slope
25	247.8 \pm 17.7	-0.77 \pm 0.04	138.0 \pm 5.9	-0.86 \pm 0.03	94.1 \pm 3.3	-1.01 \pm 0.03
5	547.3 \pm 60.1	-0.74 \pm 0.06	299.5 \pm 18.0	-0.87 \pm 0.04	268.9 \pm 18.8	-0.90 \pm 0.05
3	12.7 \pm 0.6	-0.97 \pm 0.04	9.4 \pm 0.3	-1.04 \pm 0.03	7.8 \pm 0.2	-1.20 \pm 0.03
1	7012 \pm 588	-0.76 \pm 0.05	33620 \pm 1649	-0.77 \pm 0.03	85400 \pm 4276	-1.01 \pm 0.06

Indazole **3** had previously been shown to be selective for ROR γ t over other NRs (>100-fold), with only minor cross-activity on PPAR γ .³¹ To give an indication of the cross-reactivity of the isoxazole series on PPAR γ , an HTRF coactivator recruitment assay was performed with compounds **3**, **5** and isoxazoles **19** and **23-27**. **3** and **5** show IC₅₀ values of resp. 7.2 μ M and 14.7 μ M for PPAR γ (vs. 7.8 nM and 425 nM for ROR γ t) (Table 4), meaning that they show some cross-reactivity to

PPAR γ , but still are 923- and 35-fold selective for ROR γ t. **25** and all other compounds of the isoxazole series result in only weak to no PPAR γ inhibition (IC₅₀ values >50 μ M), indicating that the isoxazole scaffold leads to favorably low PPAR cross-reactivity. Thus, these data indicate that the novel class of allosteric isoxazole inverse agonists features potential as efficacious and selective ROR γ t inverse agonists.

Table 4. IC₅₀ values observed in the competitive TR-FRET cofactor recruitment assay with PPAR γ .

Compound	IC ₅₀ (μ M)
3	7.2 \pm 0.8
5	14.7 \pm 1.0
19	78.6 \pm 5.6
23	> 100
24	> 100
25	99.3 \pm 6.4
26	> 100
27	> 100

2.6 Crystallography

Co-crystallization studies were performed for the most potent isoxazole **25** with the ROR γ t-LBD, to provide molecular insights in the ligand-receptor interaction. Crystals grew in a $P 6_1 2 2$ space group and diffracted to a resolution of 1.61 Å (Table S6). In the experimental electron density map, clear density for compound **25** is observed in the allosteric site, formed by helices 4, 5, 11 and 12 (Figure 5-A, Figure S2). The compound binds to this allosteric site in a similar orientation as **3** (Figure 5-B), as was predicted by our docking studies (Figure 3). The 2,6-disubstituted phenyl ring common to both **3** and of **25** is located in the exact same part of the binding pocket (Figure 5-B). Moreover, hydrogen-bonding interactions between the carboxylic acid group and the main-chain amide hydrogen atoms of A497 and F498, as well as with the side chain of residue Q329, are also evident in both structures. Unique to **25** is the pyrrole ring, which is oriented to allow a hydrogen bond interaction with the main-chain carbonyls of residues L353 and K354 (Figure 5-C). The isoxazole scaffold also allows a deeper penetration of this compound towards helix 4 of ROR γ t. In the case of isoxazole **25** the AF-2 loop of the protein and the allosteric ligand are positioned slightly further apart as compared to **3** (Figure 5-B). These structural data provide clear evidence for the allosteric binding of **25** to ROR γ t in an orientation that was predicted with remarkable accuracy in the docking study (Figure S3), but with specific additional molecular effects resulting from the novel isoxazole scaffold and pyrrole based substitution pattern.

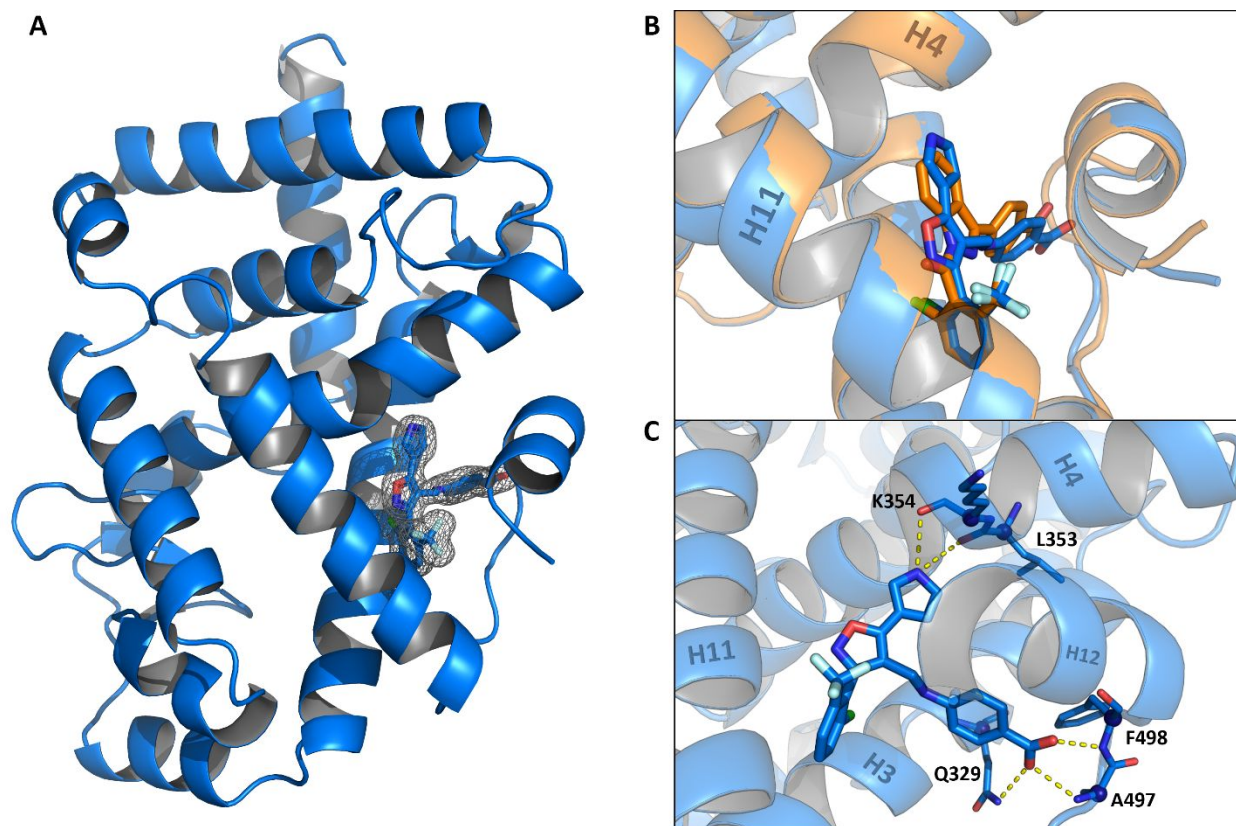


Figure 5. Co-crystal structure of RORγt with compound **25** (PDB code: 6SAL). (A) The tertiary structure of RORγt bound to **25** (stick representation). The final 2Fo - Fc electron density map of **25** is shown as an isomesh contoured at 1σ; (B) Overlay of the crystal structure of RORγt bound to **25** and RORγt bound to **3** (PDB code: 5C4O); (C) Zoom-in on the allosteric pocket of RORγt showing the interactions between **25** and the protein.

2.7 Isoxazole **25** Inhibits IL-17a Expression in EL4 Cells

EL4 is a murine lymphoblast cell line that constitutively expresses ROR γ t. Because ROR γ t promotes IL-17a production, an effective means to determine the cellular activity of ROR γ t inverse agonists is to measure the reduction in IL-17a mRNA expression levels by quantitative reverse transcriptase PCR (RT-PCR). To this end, EL4 cells were treated with 10 μ M of **3**, **25** and **23** for 24 h before IL-17a mRNA levels were measured (Figure 6). The most potent isoxazole *in vitro*, **25**, significantly reduced IL-17a mRNA expression 27-fold whilst the weaker inverse agonist **23** showed a smaller reduction (3.6-fold) compared to the DMSO control. As expected, **3** led to the most significant decrease in IL-17a expression (48-fold) which was in line with previous reports. This result demonstrates that the allosteric modulation of ROR γ t by optimized trisubstituted isoxazoles leads to an effective cellular response, correlating with the biochemical protein binding data, and which is known to be beneficial for the treatment of autoimmune disease.¹⁰⁻¹²

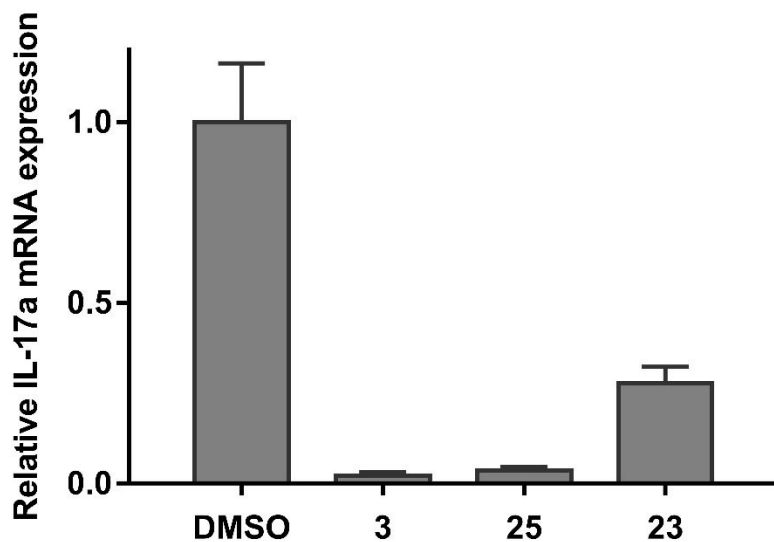


Figure 6. IL-17a mRNA expression in EL4 cells treated with ligand **3**, **25** and **23** (10 μ M, 24h) or DMSO. The level of IL-17a expression was normalized to that of GAPDH

expression. All data are expressed as the mean \pm s.d. (n=3). The relative gene expression was calculated by the $2^{-\Delta\Delta C_t}$ (Livak) method using the DMSO control as calibrator.

2.8 Absorption, Distribution, Metabolism and Excretion (ADME) Profile

To further assess the potential of **25** and isoxazole analogues such as **23** and **8** we investigated the ADME profile of these compounds, and compared them to indazole **3** (Table 5). The isoxazole compounds showed favorable profiles compared to **3** in terms of chemical stability, solubility and permeability through artificial plasma membranes (PAMPA). A metabolic stability study with human liver microsomes indicated that the 4-methylamino isoxazoles **23** and **25** were more liable to phase 1 metabolism compared to indazole **3**, which showed good stability. **23** and **25** showed promising phase 2 stability. In blood plasma, whilst inferior to **3**, the stability of **23** and **25** was acceptable, although all these compounds showed high levels of binding to plasma proteins. Pleasingly, the 5-phenyl-4-amido isoxazole **8** showed a good ADME profile, with comparable microsomal stability to **3** and reduced plasma protein binding. This likely indicates that further optimization of the C-4 and C-5 isoxazole substituents has the potential to produce candidate molecules with desirable *in vivo* efficacy.

Table 5. ADME properties for ligand **3**, **8**, **23** and **25**

Compound	Chemical Stability (% remain)	Solubility (μ M)	PAMPA (% Flux)	Microsomal Stability		Plasma stability (% remain)	Plasma protein binding (% bound)
				Phase 1	Phase 2		
				(CL _{int} ,	(% remain)		

$\mu\text{L}/\text{min}/\text{mg}$								
)								
3	81.0	390	23.7	−1.2	47.1	100	99.9	
8	95.4	490	60.1	−0.1	100	99.9	97.8	
23	100	392	50.4	43.2	92.8	86.5	100	
25	95.3	411	33.6	20.7	69.8	85.9	99.9	

3. CONCLUSIONS

To summarize, we report the design, synthesis and early optimization of a novel class of ROR γ t allosteric inverse agonists. The chemotype of the central aromatic ring system differs significantly from all the other fused bicyclic ring systems reported thus far. To identify this novel, more diverse, molecular scaffold we used the crystal structure of **3** bound to the ROR γ t allosteric site as the basis for a 3D pharmacophore screen against a virtual compound library. Rational design steps led to the discovery of the *in silico* designed hit **8**, which already featured a modest inhibition of transcriptional coactivator recruitment to the ROR γ t LBD and served as starting point for further optimization in a SAR campaign. A second and highly efficient iteration of lead optimization was guided by *in silico* docking. Through the synthesis of just five derivatives (Table 2), this process delivered **25**, a sub-micromolar allosteric inverse agonist. It is highly noteworthy that there was a strong correlation between the Glide dockings scores and the ROR γ t biochemical activity within this new class of isoxazole. Whereas screening approaches do not overtly identify allosteric ligands, our rational scaffold hopping approach is much more targeted, with less demand on experimental resource. Overall, the discovery workflow adopted, with a central role for structure-driven *in silico* screening and optimization, showed to be highly effective and might have wider application in expediting NR allosteric drug discovery.

Competitive coactivator recruitment and ligand binding assays were used to confirm the allosteric mode-of-action, with concomitant cooperative ROR γ t binding with an inverse agonist. This was also shown for thienopyrazole **5**, having not previously been disclosed. The co-crystal structure of **25** in complex with the ROR γ t LBD unequivocally proved the allosteric binding mode, via a similar mechanism to **3** and was impressively similar to the initially docked structure of **25** in ROR γ t. The co-crystal of **25** with the ROR γ t LBD revealed a number of unique interactions and structural ROR γ t modifications that bring forward intriguing insights and new lines of exploration regarding ROR γ t allosteric ligand binding, selectivity, and affinity optimization, which are currently explored. Compound **25** was shown to significantly reduce IL-17a mRNA expression in EL4 cells and to have a promising ADME profile. These factors highlight the potential of this new isoxazole-based ligand class and overt targeting of the ROR γ t allosteric site to deliver effective treatments for autoimmune diseases.

4. EXPERIMENTAL SECTION

4.1. Pharmacophore Screening. The receptor-ligand complex structure (PDB code: 4YPQ) was prepared using the Protein Preparation Wizard within Maestro (version 2017-2, Schrödinger LLC, New York, NY, USA) (default parameters). A 3D pharmacophore model for **3** bound to the allosteric pocket of ROR γ t LBD was created using Phase (version 2017-2, Schrödinger LLC, default hypothesis settings). Energy minimized 3D ligand conformations for each molecule to be investigated were generated using the Ligand Preparation wizard within Maestro (default parameters). These were screened against the hypothesis whereby up to 50 ligand conformations were generated for each molecule. A hit was returned for compounds that matched 4 out of 6 pharmacophore features and these were ranked using the Phase Screen Score. The structure and ranking for the top 30 hits identified from the Asinex Gold Platinum library can be found in the Supporting Information.

4.2. Molecular Docking Studies. The receptor-ligand structure (PDB code: 4YPQ) was prepared as described above. A receptor grid centered on the bound ligand was created using Glide (version 2017-2, Schrödinger LLC). All parameters were kept as the default.

Ligand libraries were either enumerated in SMILES format using the open-access ChemT software, or generated manually (see Supporting Information). Ligands were prepared using the Ligand Preparation wizard as described above. Ligands were docked using Glide (version 2017-2, Schrödinger LLC) in standard precision mode with flexible ligand sampling. The predicted binding modes of all ligands were ranked according to their Glide Score (see Supporting Information for selected examples).

4.3. General Chemistry. All non-aqueous reactions were performed under an argon atmosphere unless otherwise stated. Water-sensitive reactions were performed in oven-dried glassware, cooled under argon before use. Solvents were removed *in vacuo* using a Büchi rotary evaporator and a diaphragm pump. THF and CH₂Cl₂ were dried and purified by means of a MBRAUN Solvent Purification System (MB-SPS-800). Anhydrous DMF was obtained in SureSeal bottles from Sigma-Aldrich. All other solvents used were of chromatography or analytical grade and supplied by Biosolve or Sigma-Aldrich. Commercially available starting materials were obtained from Sigma-Aldrich, Fluka, Acros, Alfa-Aesar or Fluorochem and were used without further purification unless stated. TLC was carried out on aluminium-backed silica (Merck silica gel 60 F254) plates

supplied by Merck. Visualization of the plates was achieved using an ultraviolet lamp ($\lambda_{\text{max}} = 254 \text{ nm}$), KMnO_4 , anisaldehyde or ninhydrin. Column chromatography was either performed manually using silica gel (60-63 μm particle size) or using an automated Grace Reveleris X2 chromatograph with pre-packed silica columns supplied by Buchi/Grace (40 μm particle size). LCMS analysis was carried out with a system comprising a Thermo Fischer LCQ Fleet Ion Trap Mass Spectrometer and C18 Jupiter SuC4300A 150 x 2.0 mm column using a gradient of 5-100% MeCN in water (+ 0.1% HCOOH) over 15 minutes. The purity of the samples was assessed using a UV detector at 254 nm. Unless otherwise stated all final compounds were >95% pure as judged by HPLC. GCMS analysis was performed on a Phenomenex Zebron ZB-5MS 30 m x 0.25 mm x 0.25 mm column with a gradient of 80 $^{\circ}\text{C}$ for 1 min. to 300 $^{\circ}\text{C}$ for 1 min. with a rate of 30 $^{\circ}\text{C}/\text{min}$. in helium gas connected to a GCMS-QP2010 Plus Quadrupole Mass Spectrometer. High resolution mass spectra (HRMS) were recorded using a Waters ACQUITY UPLC I-Class LC system coupled to a Xevo G2 Quadrupole Time of Flight (Q-tof) mass spectrometer. Proton (^1H) and carbon (^{13}C) NMR spectral data were collected on a 400 MHz Bruker Cryomagnet or 400 MHz Varian Gemini. Chemical shifts (δ) are quoted in parts per million (ppm) and referenced to the residual solvent peak. Coupling constants (J) are quoted in Hertz (Hz) and splitting patterns reported in an abbreviated

manner: app. (apparent), s (singlet), d (doublet), t (triplet), q (quartet), m (multiplet).

Assignments were made with the aid of 2D COSY, HMQC and HMBC experiments.

4.3.1. General Procedure for Ester Hydrolysis. LiOH.H₂O (5.0 eq) was added to a suspension of ester (1.0 eq) in a 4:1 mixture of MeOH-H₂O (0.2 M). The reaction mixture was heated to 70 °C until TLC analysis indicated complete consumption of the starting material. MeOH was removed *in vacuo* and the resulting aqueous mixture was acidified to pH 3 using 10% v/v aqueous HCl and extracted with a 9:1 mixture of CH₂Cl₂-MeOH (x 5). The combined organic phase was dried (MgSO₄), filtered and concentrated *in vacuo* to furnish an ester which was purified as described.

4.3.2. General Procedure for Amide Coupling. Carboxylic acids (1.0 eq) were dissolved in SOCl₂ (50 eq) and heated to 50 °C for 2 h. The excess SOCl₂ was removed *in vacuo* to furnish an acid chloride intermediate that was immediately dissolved in CH₂Cl₂ (0.1 M). To this was added NEt₃ (3.0 eq), the appropriate amine or aniline (1.5 eq) and DMAP (0.1 eq) and the reaction mixture was stirred at reflux for 18 h. The reaction mixture was diluted with saturated aqueous NH₄Cl solution and extracted with ethyl acetate (3 x). The combined organic phase was washed with brine, dried over MgSO₄, filtered and

concentrated *in vacuo*. The crude product was purified by flash column chromatography (SiO₂) using the specified eluent.

4.3.3. General Procedure for tert-Butyl Ester Deprotection. Esters (1.0 eq) were treated with a 20% trifluoroacetic acid solution in CH₂Cl₂ (0.2 M). The reaction mixture was stirred at the specified temperature for the specified amount of time and then concentrated *in vacuo*. The crude product was purified as indicated.

4.3.4. General Procedure for Suzuki Coupling. Under an inert atmosphere the pinacol boronate (2.0 eq), Cs₂CO₃ (2.0 eq) and Pd(dppf)Cl₂ (0.1 eq) were added to a solution of bromide **30a** (1.0 eq) in de-gassed DME. The reaction mixture was heated at 85 °C for 8 h, cooled to room temperature, diluted with saturated aqueous NH₄Cl and extracted with EtOAc (3 x). The combined organic phase was dried (MgSO₄), filtered and concentrated *in vacuo*. The crude product was purified by flash column chromatography using the specified eluent.

4.3.5. General Procedure for Conversion of Esters to Aldehydes. LiAlH₄ (1 M in THF, 1.0 eq) was added dropwise to a solution of ester (1.0 eq) in THF (0.2 M) at 0 °C. The reaction mixture was warmed to room temperature and stirred until TLC analysis indicated

complete consumption of the starting material. The reaction mixture was cooled to 0 °C, quenched by the addition of saturated aqueous NH₄Cl solution and extracted with EtOAc (3 x). The combined organic phase was dried (MgSO₄), filtered and concentrated *in vacuo*. The resulting intermediate product was dissolved in CH₂Cl₂ (0.2 M). To this was added Dess-Martin Periodinane (1.5 eq) and the reaction mixture was stirred at room temperature until TLC analysis indicated complete consumption of the intermediate. The reaction mixture was quenched by the addition of 10% aqueous Na₂S₂O₃ solution and extracted with CH₂Cl₂ (3 x). The combined organic phase was washed with saturated aqueous NaHCO₃ and H₂O, dried (MgSO₄), filtered and concentrated *in vacuo* to furnish the title compound which was purified as described.

4.3.6. General Procedure for Reductive Amination. The chosen amine or aniline (1.0 eq) was added to a solution of the appropriate aldehyde (1.0 eq) and AcOH (0.1 eq) in MeOH or EtOH (0.25 M). The reaction mixture was heated at reflux for 24 h and then concentrated *in vacuo*. The intermediate imine was isolated by flash column chromatography using the specified eluent and then dissolved in MeOH or EtOH (0.2 M), cooled to 0 °C (ice) and treated with NaBH₄ (5.0 eq). The reaction mixture was held at the

specified temperature until TLC analysis indicated complete consumption of the imine.

The solvent was removed *in vacuo* and the mixture was dissolved in CH₂Cl₂ and washed with water. The aqueous phase was further extracted with CH₂Cl₂ (2 x), dried (MgSO₄), filtered and concentrated *in vacuo*. The crude product was purified by flash column chromatography (SiO₂) using the specified eluent.

4.3.7. 4-{3-[2-Chloro-6-(trifluoromethyl)phenyl]-5-methyl-1,2-oxazole-4-amido}benzoic acid (7). According to the General Procedure for amide coupling carboxylic acid **11a** (60.0 mg, 0.199 mmol) was coupled with *tert*-butyl-4-amino benzoate. The crude product was purified by flash column chromatography, eluting with 20% EtOAc in cyclo-hexane, to furnish the amide (46.0 mg, 48%). The intermediate product (43.0 mg, 0.089 mmol) was subject to *tert*-butyl ester deprotection (see General Procedure for *tert*-Butyl ester deprotection) and purified by trituration with Et₂O to furnish **7** (33.0 mg, 87%) as a colourless solid. *R*_f = 0.52 (9:1 CH₂Cl₂-MeOH); ¹H-NMR (400 MHz, MeOD): δ (ppm) 7.97 (2 H, d, *J* = 8.8, benzoate H-2), 7.81 (2 H, app. d, *J* = 8.0, Ar H-3 and Ar H-5), 7.67 (1 H, t, *J* = 8.0, Ar H-4), 7.61 (2 H, d, *J* = 8.8, benzoate H-3), 2.76 (3 H, s, CH₃); ¹³C-NMR (100 MHz, MeOD): δ (ppm) 171.3 (C-5), 161.2 (CO₂H), 159.5 (C-3), 143.8 (benzoate C-4),

137.4 (ArC-2), 134.4 (ArC-3), 132.7 (q, $J = 30.9$, ArC-6), 132.6 (ArC-4), 131.8 (benzoate C-2), 127.6 (ArC-1), 127.5 (benzoate C-1), 126.1 (q, $J = 5.1$, ArC-5), 120.6 (benzoate C-3), 116.1 (C-4), 12.8 (CH_3); LC-MS (ESI): calc. for $\text{C}_{19}\text{H}_{13}\text{ClF}_3\text{N}_2\text{O}_4$ $[\text{M}+\text{H}]^+$: 425.04, observed: 425.17, LC R_t : 6.22 min. HRMS (ESI): calc. for $\text{C}_{19}\text{H}_{13}\text{ClF}_3\text{N}_2\text{O}_4$ $[\text{M}+\text{H}]^+$: 425.0516, observed: 425.0511.

4.3.8. 4-{3-[2-Chloro-6-(trifluoromethyl)phenyl]-5-phenyl-1,2-oxazole-4-amido}benzoic acid (8). *tert*-Butyl benzoate **14** (30.0 mg, 0.055 mmol) was deprotected according to the General Procedure for *tert*-Butyl ester deprotection. The crude product was purified by trituration with Et_2O to furnish **8** (21.0 mg, 78%) as a colourless solid. $R_f = 0.55$ (9:1 CH_2Cl_2 -MeOH); ^1H -NMR (400 MHz, $\text{DMSO}-d_6$): δ (ppm) 7.97 (1 H, d, $J = 8.2$, ArH-3 or ArH-5), 7.92 (1 H, d, $J = 7.9$, ArH-3 or ArH-5), 7.85-7.83 (4 H, m, benzoate H-2, PhH-ortho), 7.78 (1 H, app. t, $J = 8.1$, ArH-4), 7.58-7.54 (5 H, m, benzoate H-3, PhH-meta, PhH-para); ^{13}C -NMR (100 MHz, CDCl_3): δ (ppm) 167.0 (C-5), 166.8 (CO_2H), 158.9 (CO_2NH), 158.7 (C-3), 142.3 (benzoate C-4), 135.5 (ArC-2), 133.7 (ArC-3), 132.4 (PhC-quart.), 131.6 (ArC-4), 130.6 (ArC-6), 130.3 (benzoate C-2), 129.4 (PhC-ortho), 127.3 (PhC-meta), 126.0 (PhC-para), 125.9 (benzoate C-1), 125.3 (ArC-5 and ArC-1), 119.3 (benzoate C-3), 113.4

(C-4), quartet for CF_3 not observed; LC-MS (ESI): calc. for $\text{C}_{24}\text{H}_{15}\text{ClF}_3\text{N}_2\text{O}_4$ $[\text{M}+\text{H}]^+$: 487.06, observed: 487.17, LC R_t : 7.00 min. HRMS (ESI): calc. for $\text{C}_{24}\text{H}_{15}\text{ClF}_3\text{N}_2\text{O}_4$ $[\text{M}+\text{H}]^+$: 487.0672, observed: 487.0662.

4.3.9. (E)-N-[[2-Chloro-6-(trifluoromethyl)phenyl]methylidene]hydroxylamine (9).

Hydroxylamine hydrochloride (3.95 g, 57.0 mmol, 1.2 eq) was suspended in EtOH (20 mL) and 10% w/v aqueous solution of NaOH (20 mL) was added such that the final pH of the resulting solution was < pH 9. 2-Chloro-6-(trifluoromethyl)benzaldehyde (9.88 g, 47.4 mmol, 1.0 eq) was then added as a solution in EtOH (20 mL) and the mixture was stirred at room temperature for 18 h. The reaction mixture was diluted with H_2O (100 mL) and extracted with CH_2Cl_2 (3 x 100 mL). The combined organic phase was dried (MgSO_4), filtered and concentrated *in vacuo* to furnish **9** (8.77 g, 83%) as a colourless solid which was used without further purification. R_f = 0.45 (4:1 c-hexane-EtOAc); ^1H -NMR (400 MHz, CDCl_3): δ (ppm) 8.97 (1H, s, $\text{N}=\text{CH}$), 8.36 (1H, s, NOH), 7.67-7.64 (2 H, m, H-3, H-5), 7.45 (1 H, app. t, J = 8.0, H-4); ^{13}C -NMR (100 MHz, CDCl_3): δ (ppm) 145.3 ($\text{N}=\text{CH}$), 135.7 (C-2), 133.6 (C-3), 131.3 (q, J = 31.2, C-6), 130.2 (C-4), 129.0 (C-1), 125.1 (q, J = 5.5, C-5), 123.22 (q, J = 274.2, F_3C); LC-MS (ESI): calc. for $\text{C}_8\text{H}_6\text{ClF}_3\text{NO}$ $[\text{M}+\text{H}]^+$: 224.00, observed: 224.00, LC R_t : 5.82 min.

4.3.10. (Z)-2-Chloro-N-hydroxy-6-(trifluoromethyl)benzene-1-carbonimidoyl chloride

(9a). *N*-Chlorosuccinamide (5.22 g, 39.1 mmol, 1.0 eq) was added to a solution of hydroxylamine **9** (8.74 g, 39.1 mmol, 1.0 eq) in DMF (80 mL). The reaction mixture was stirred at 60 °C for 18 h then diluted with H_2O (150 mL) and extracted with Et_2O (3 x 100 mL). The combined organic

phase was washed with H₂O (3 x 100 mL) and brine (100 mL), dried (MgSO₄), filtered and concentrated *in vacuo* to furnish **9a** (9.10 g, 95% purity, 86%) which was used immediately in the next step without further purification. R_f = 0.42 (4:1 c-hexane-EtOAc); ¹H-NMR (400 MHz, CDCl₃): δ (ppm) 8.50 (1H, s, NOH), 7.68-7.66 (2 H, m, H-3, H-5), 7.53 (1 H, app. t, J = 8.1, H-4).

4.3.11. Ethyl 3-[2-chloro-6-(trifluoromethyl)phenyl]-5-methyl-1,2-oxazole-4-carboxylate

(10a). NEt₃ (0.570 mL, 4.07 mmol, 2.5 eq) was added to a solution of imidoyl chloride **9a** (0.421 g, 1.63 mmol, 1.0 eq) in THF (2.5 mL). A white precipitate formed immediately after which was added ethyl 2-butyrate (0.190 mL, 1.63 mmol, 1.0 eq). The reaction mixture was heated to reflux for 4 h, filtered and concentrated *in vacuo*. The crude material was purified by automated flash column chromatography, eluting with a gradient of 2-5% EtOAc in c-hexane, to furnish **10a** (0.375 g, 69%) as a colourless oil. R_f = 0.22 (9:1 c-hexane-EtOAc); ¹H-NMR (400 MHz, CDCl₃): δ (ppm) 7.69 (1 H, d, J = 8.0, ArH-3 or ArH-5), 7.66 (1 H, d, J = 8.0, ArH-3 or ArH-5), 7.53 (1 H, app. t, J = 8.0, ArH-4); 4.07 (2 H, 2x dq (overlapping), J = 12.7, 7.1, CO₂CH₂CH₃), 2.78 (3 H, s, CH₃), 0.98 (3 H, t, J = 7.1, OCH₂CH₃); ¹³C-NMR (100 MHz, CDCl₃): δ (ppm) 175.4 (C-5), 161.1 (CO₂Et), 158.1 (C-3), 136.3 (ArC-2), 132.7 (ArC-3), 131.6 (q, J = 31.6, ArC-6), 130.6 (ArC-4), 127.5 (ArC-1), 124.6 (q, J = 5.0, ArC-5), 123.0 (q, J = 274.5, F₃C), 110.2 (C-4), 60.6 (OCH₂CH₃), 13.66 (CH₃), 13.3 (OCH₂CH₃); LC-MS (ESI): calc. for C₁₄H₁₂ClF₃NO₃ [M+H]⁺: 334.04, observed: 334.08, LC R_t: 7.47 min.

4.3.12. Ethyl 3-[2-chloro-6-(trifluoromethyl)phenyl]-5-phenyl-1,2-oxazole-4-carboxylate

(10b). NEt₃ (3.92 mL, 28.1 mmol, 2.5 eq) was added to a solution of imidoyl chloride **9a**

(2.90 g, 11.3 mmol, 1.0 eq) in THF (17 mL). A white precipitate formed immediately after which was added ethyl-3-phenyl propionate (1.85 mL, 11.3 mmol, 1.0 eq). The reaction mixture was heated to reflux for 6 h, filtered and concentrated *in vacuo*. The crude material was purified by automated flash column chromatography, eluting with a gradient of 0-25% EtOAc in n-heptane, to furnish **10b** (3.59 g, 80%) as a colourless solid. $R_f = 0.47$ (4:1 c-hexane-EtOAc); $^1\text{H-NMR}$ (400 MHz, CDCl_3): δ (ppm) 8.16-8.13 (2 H, m, PhH-ortho), 7.74 (1 H, d, $J = 7.9$, ArH-3 or ArH-5), 7.71 (1 H, d, $J = 8.2$, H-3 or H-5), 7.59-7.51 (4 H, m, H-4, Ar-H), 4.06 (2 H, dq (2 overlapping), $J = 11.8, 7.1$, $\text{CO}_2\text{CH}_2\text{CH}_3$), 0.88 (3 H, t, $J = 7.1$, OCH_2CH_3); $^{13}\text{C-NMR}$ (100 MHz, CDCl_3): δ (ppm) 173.0 (C-5), 160.8 (CO_2Et), 159.2 (C-3), 136.3 (ArC-2), 132.6 (ArC-3), 131.7 (PhC-quart.), 131.5 (q, $J = 30.5$, ArC-6), 130.5 (ArC-4), 129.2 (PhC-ortho), 128.5 (PhC-meta), 127.8 (q, $J = 1.8$, ArC-1), 126.3 (PhC-meta), 124.5 (q, $J = 5.0$, ArC-5), 122.9 (q, $J = 274.3$, F_3C), 109.3 (C-4), 60.8 (OCH_2CH_3), 13.3 (OCH_2CH_3); LC-MS (ESI): calc. for $\text{C}_{19}\text{H}_{14}\text{ClF}_3\text{NO}_3$ $[\text{M}+\text{H}]^+$: 396.06, observed: 396.17, LC R_t : 8.40 min.

4.3.13. 3-[2-Chloro-6-(trifluoromethyl)phenyl]-5-methyl-1,2-oxazole-4-carboxylic acid (11a). According to the General Procedure for ester hydrolysis, ester **10a** (0.273 g, 0.820

mmol) was hydrolyzed in 8 h to furnish **11a** (0.210 g, 84%) as a colourless solid which required no further purification. R_f = 0.61 (EtOAc); $^1\text{H-NMR}$ (400 MHz, DMSO- d_6): δ (ppm) 13.09 (1 H, br. s, CO_2H), 7.96 (1 H, d, J = 8.0, ArH-3 or ArH-5), 7.90 (1 H, d, J = 8.0, ArH-3 or ArH-5), 7.77 (1 H, app. t, J = 8.0, ArH-4), 2.76 (3 H, s, CH_3); $^{13}\text{C-NMR}$ (100 MHz, DMSO- d_6): δ (ppm) 175.3 (C-5), 161.9 (CO_2H), 158.2 (C-3), 135.3 (ArC-2), 133.4 (ArC-3), 131.8 (ArC-4), 130.1 (q, J = 30.8, ArC-6), 126.8 (ArC-1), 125.1 (q, J = 5.0, ArC-5), 123.0 (q, J = 274.4, F_3C), 110.5 (C-4), 12.8 (CH_3); LC-MS (ESI): calc. for $\text{C}_{12}\text{H}_6\text{ClF}_3\text{NO}_3$ $[\text{M-H}]^-$: 304.01, observed: 304.17, LC R_t : 5.82 min.

4.3.14. 3-[2-Chloro-6-(trifluoromethyl)phenyl]-5-phenyl-1,2-oxazole-4-carboxylic acid (11b). According to the General Procedure for ester hydrolysis, ester **10b** (3.66 g, 9.26 mmol) was hydrolyzed in 8 h to furnish **11b** (3.25 g, 95%) as a colourless solid which required no further purification. R_f = 0.35 (1:1 c-hexane-EtOAc); $^1\text{H-NMR}$ (400 MHz, CDCl_3): δ (ppm) 8.05-8.03 (2 H, m, PhH-ortho), 7.71 (1 H, d, J = 8.0, ArH-3 or ArH-5), 7.68 (1 H, d, J = 8.1, H-3 or H-5), 7.60-7.50 (4 H, m, H-4, Ar-H); $^{13}\text{C-NMR}$ (100 MHz, DMSO- d_6): δ (ppm) 171.8 (C-5), 161.5 (CO_2H), 159.3 (C-3), 135.2 (ArC-2), 133.4 (ArC-3), 132.0 (PhC-quart.), 131.8 (ArC-4), 130.0 (q, J = 30.5, ArC-6), 129.0 (PhC-ortho), 128.7 (PhC-

meta), 126.7 (ArC-1), 125.7 (PhC-meta), 125.2 (q, $J = 5.0$, ArC-5), 123.0 (q, $J = 274.4$, F_3C), 99.4 (C-4); LC-MS (ESI): calc. for $C_{17}H_{10}ClF_3NO_3$ $[M+H]^+$: 368.02, observed: 368.08, LC retention time: 7.03 min. HRMS (ESI): calc. for $C_{17}H_{10}ClF_3NO_3$ $[M+H]^+$: 368.0301, observed: 368.0299.

4.3.15. 3-[2-Chloro-6-(trifluoromethyl)phenyl]-5-phenyl-1,2-oxazole-4-carbaldehyde (12). Carboxylic acid **11b** (2.0 g, 5.44 mmol, 1.0 eq) was dissolved in $SOCl_2$ (10.0 mL, 138 mmol, 25 eq) and heated to 60 °C for 2 h. Excess $SOCl_2$ was removed *in vacuo* and the intermediate acid chloride was immediately dissolved in CH_2Cl_2 (20 mL) and cooled to 0 °C. To this was added NEt_3 (2.27 mL, 16.3 mmol, 3.0 eq) and *N,O*-dimethyl hydroxylamine hydrochloride (0.580 g, 5.98 mmol, 1.1 eq). The reaction mixture was allowed to warm to room temperature with stirring over 16 h before being quenched by the addition of saturated aqueous NH_4Cl solution and extracted with CH_2Cl_2 (3 x 20 mL). The combined organic phase was dried ($MgSO_4$), filtered and concentrated *in vacuo*. The resulting Weinreb amide was dissolved in THF (20 mL) and cooled to 0 °C. To this was added $LiAlH_4$ (1 M in THF, 2.72 mL, 2.72 mmol, 0.5 eq) and the reaction mixture was stirred at 0 °C for 1 h before being quenched by the addition of saturated aqueous NH_4Cl solution

(20 mL) and extracted with EtOAc (3 x 20 mL). The combined organic phase was dried (MgSO₄), filtered and concentrated *in vacuo* to furnish a crude product which was purified by automated flash column chromatography, eluting with a gradient of 10-30% EtOAc in n-heptane, to furnish **12** (1.25 g, 65%) as a colourless solid. R_f = 0.65 (1:1 c-hexane-EtOAc); ¹H-NMR (400 MHz, CDCl₃): δ (ppm) 9.93 (1 H, s, CHO), 8.06-8.04 (2 H, m, PhH-ortho), 7.77 (1 H, d, J = 7.9, ArH-3 or ArH-5), 7.74 (1 H, d, J = 7.8, ArH-3 or ArH-5), 7.68-7.59 (4 H, m, H-4, PhH); ¹³C-NMR (100 MHz, CDCl₃): δ (ppm) 182.8 (CHO), 174.6 (C-5), 160.8 (CO₂Et), 158.6 (C-3), 136.3 (ArC-2), 133.2 (ArC-3), 132.7 (PhC-quart.), 132.0 (q, J = 30.9, ArC-6), 131.3 (ArC-4), 129.5 (PhC-ortho), 128.9 (PhC-meta), 125.9 (ArC-1), 125.7 (PhC-para), 125.0 (ArC-5), 123.0 (q, J = 274.9, F₃C), 116.2 (C-4); LC-MS (ESI): calc. for C₁₇H₁₀ClF₃NO₂ [M+H]⁺: 352.03, observed: 352.08, LC R_t: 7.28 min.

4.3.16. 3-[2-Chloro-6-(trifluoromethyl)phenyl]-5-phenyl-1,2-oxazol-4-amine (13). NEt₃ (0.760 mL, 5.44 mmol, 1.1 eq) and diphenylphosphoryl azide (1.06 mL, 4.95 mmol, 1.0 eq) were added to a pre-warmed solution of acid **11b** (1.82 g, 4.95 mmol, 1.0 eq) in *t*-BuOH (18 mL) at 50 °C. The reaction mixture was then heated to 85 °C for 18 h after which it was cooled to room temperature and diluted with 1 M aqueous HCl (50 mL) and

1
2
3 extracted with EtOAc (3 x 30 mL). The combined organic phase was washed with
4
5
6
7 saturated aqueous NaHCO₃ (100 mL) and brine (100 mL), dried (MgSO₄), filtered and
8
9
10 concentrated *in vacuo*. The crude product was purified by automated flash column
11
12
13 chromatography, eluting with a gradient of 0-20% EtOAc in n-heptane, to furnish a
14
15
16 carbamate (1.41 g, 65%) as a colourless solid. Trifluoroacetic acid (3.0 mL) was added
17
18
19 to a solution of the carbamate (1.13 g, 2.58 mmol, 1.0 eq) in CH₂Cl₂ (9.0 mL). The reaction
20
21
22
23
24 mixture was heated at reflux for 4 h then cooled to room temperature and concentrated
25
26
27 *in vacuo*. The crude product was dissolved in CH₂Cl₂ (100 mL) and washed with saturated
28
29
30 aqueous NaHCO₃ (100 mL) and water (100 mL), dried (MgSO₄), filtered and concentrated
31
32
33 *in vacuo* to furnish **13** (0.798 g, 91%) as a pale yellow solid that was used without further
34
35
36 purification. *R*_f = 0.56 (1:1 c-hexane-EtOAc); ¹H-NMR (400 MHz, CDCl₃): δ (ppm) 7.86 (1
37
38
39 H, d, *J* = 7.0, ArH-3 or ArH-5), 7.79-7.76 (2 H, m, PhH-ortho), 7.61 (1 H, app. t, *J* = 8.0,
40
41
42 ArH-3 or ArH-5), 7.54-7.49 (3 H, m, PhH), 7.41 (1 H, app. t, *J* = 8.0, ArH-4), 2.97 (2 H, s,
43
44
45 NH₂); ¹³C-NMR (100 MHz, CDCl₃): δ (ppm) 164.5 (C-5), 154.7 (C-3), 137.0 (ArC-2), 133.4
46
47
48 (ArC-3), 131.4 (PhC-quart.), 129.1 (PhC-ortho), 128.9 (ArC-4), 128.3 (PhC-para), 126.5
49
50
51 (ArC-5), 126.0 (q, *J* = 4.0, ArC-1), 125.2 (PhC-meta), 122.9 (q, *J* = 274.4, CF₃), 110.4 (C-

4); LC-MS (ESI): calc. for $C_{16}H_{11}ClF_3N_2O$ $[M+H]^+$: 339.04, observed: 339.08, LC R_t : 7.12 min.

4.3.17. tert-Butyl 4-{3-[2-chloro-6-(trifluoromethyl)phenyl]-5-phenyl-1,2-oxazole-4-amido}benzoate (14). According to the General Procedure for amide coupling, carboxylic acid **11b** (0.200 g, 0.540 mmol) was coupled with *tert*-butyl-4-amino benzoate. The crude product was purified by flash column chromatography, eluting with 15% EtOAc in *c*-hexane, to furnish amide **14** (0.260 g, 88%) as a colourless solid. R_f = 0.55 (3:2 *c*-hexane-EtOAc); 1H -NMR (400 MHz, $CDCl_3$): δ (ppm) 7.96 (2 H, dd, J = 7.9, 1.7, PhH-ortho), 7.86 (2 H, d, J = 8.7, benzoate H-2), 7.77 (2 H, app. t, J = 8.1, ArH-3 and ArH-5), 7.63-7.56 (4 H, m, PhH-meta, PhH-para, ArH-4), 7.37 (1 H, br. s, $C(O)NH$), 7.29 (2 H, d, J = 8.7, benzoate H-3), 1.55 (9 H, s, $CO_2C(CH_3)_3$); ^{13}C -NMR (100 MHz, $CDCl_3$): δ (ppm) 169.4 (C-5), 165.1 (CO_2H), 158.4 (C-3 and CO_2NH), 140.8 (benzoate C-4), 136.6 (ArC-2), 133.3 (ArC-3), 132.1 (PhC-quart.), 131.5 (ArC-4), 130.7 (ArC-6), 129.5 (PhC-ortho and benzoate C-2), 128.7 (PhC-meta), 128.2 (benzoate C-1), 126.2 (ArC-1), 126.0 (PhC-para), 125.1 (ArC-5), 118.7 (benzoate C-3), 113.0 (C-4), 81.1 ($CO_2C(CH_3)_3$), 28.3 ($CO_2C(CH_3)_3$, quartet for CF_3 not observed; LC-MS (ESI): calc. for $C_{28}H_{23}ClF_3N_2O_4$

[M+H]⁺: 543.12, observed: 543.08, LC R_t: 8.88 min. HRMS (ESI): calc. for

C₂₈H₂₃ClF₃N₂O₄ [M+H]⁺: 543.1298, observed: 543.1292.

4.3.18. 2-(4-{3-[2-Chloro-6-(trifluoromethyl)phenyl]-5-phenyl-1,2-oxazole-4-amido}phenyl) acetic acid (15). According to the General Procedure for amide coupling, carboxylic acid **11b** (0.200 g, 0.540 mmol) was coupled with methyl-(4-aminophenyl) acetate. The crude product was purified by flash column chromatography, eluting with a gradient of 15% - 45% EtOAc in n-heptane, to furnish the amide (0.173 g, 62%). The intermediate product (0.117 g, 0.230 mmol) was subject to ester hydrolysis according to the General Procedure for ester hydrolysis and purified by trituration with Et₂O to furnish **15** (0.099 g, 87%) as a colourless solid. *R_f* = 0.55 (9:1 CH₂Cl₂-MeOH); ¹H-NMR (400 MHz, DMSO-d₆): δ (ppm) 12.32 (1 H, br. s, CO₂H), 10.49 (1 H, s, CONH), 7.98 (1 H, d, *J* = 8.2, ArH-3 or ArH-5), 7.93 (1 H, d, *J* = 8.0, ArH-3 or ArH-5), 7.88-7.87 (2 H, m, PhH-ortho), 7.79 (1 H, app. t, *J* = 8.1, ArH-4), 7.61-7.59 (3 H, m, PhH-meta, PhH-para), 7.40 (2 H, d, *J* = 8.2, benzoate H-2), 7.15 (2 H, d, *J* = 8.2, benzoate H-3), 3.49 (2 H, br. s, benzylic CH₂); ¹³C-NMR (100 MHz, DMSO-d₆): δ (ppm) 172.7 (CO₂H), 166.6 (C-5), 158.7 (CO₂NH), 158.4 (C-3), 136.9 (benzoate C-4), 135.5 (ArC-2), 133.6 (ArC-3), 132.3 (PhC-

quart.), 131.4 (ArC-4), 130.9 (benzoate C-1), 130.5 (q, $J = 30.9$, ArC-6), 129.7 (benzoate C-2), 129.4 (PhC-ortho), 127.2 (PhC-meta), 126.0 (PhC-para), 125.5 (ArC-5), 125.3 (ArC-1), 122.9 (q, $J = 274.5$, CF_3), 119.9 (benzoate C-3), 113.8 (C-4), 30.7 (benzylic CH_2); LC-MS (ESI): calc. for $\text{C}_{25}\text{H}_{17}\text{ClF}_3\text{N}_2\text{O}_4$ $[\text{M}+\text{H}]^+$: 501.08, observed: 501.17, LC R_t : 6.67 min. HRMS (ESI): calc. for $\text{C}_{25}\text{H}_{17}\text{ClF}_3\text{N}_2\text{O}_4$ $[\text{M}+\text{H}]^+$: 501.0829 observed: 501.0829.

4.3.19. 3-{3-[2-Chloro-6-(trifluoromethyl)phenyl]-5-phenyl-1,2-oxazole-4-amido}benzoic acid (16). According to the General Procedure for amide coupling, carboxylic acid **11b** (0.200 g, 0.540 mmol) was coupled with methyl-3-amino benzoate. The crude product was purified by flash column chromatography, eluting with 15% EtOAc in c-hexane, to furnish the amide (0.212 g, 78%). The intermediate product (0.100 g, 0.200 mmol) was subject to ester hydrolysis according to the General Procedure for ester hydrolysis and purified by trituration with Et_2O to furnish **16** (0.070 g, 72%) as a colourless solid. $R_f = 0.51$ (9:1 CH_2Cl_2 -MeOH); $^1\text{H-NMR}$ (400 MHz, DMSO-d_6): δ (ppm) 13.01 (1 H, br. s, CO_2H), 10.66 (1 H, s, CONH), 8.11 (1 H, s, benzoate H-2), 7.98 (1 H, d, $J = 8.1$, ArH-3 or ArH-5), 7.91 (1 H, d, $J = 7.7$, ArH-3 or ArH-5), 7.87 (2 H, m, PhH-ortho), 7.80 (1 H, app. t, $J = 8.0$, ArH-4), 7.68-7.64 (2 H, m, benzoate H-4 and H-6), 7.63-7.59 (3 H, m,

PhH-meta, PhH-para), 7.40 (1 H, app. t, $J = 7.8$, benzoate H-5); ^{13}C -NMR (100 MHz, DMSO- d_6): δ (ppm) 166.9 (C-5), 158.7 (CO_2H), 158.6 (CO_2NH), 154.5 (C-3), 138.5 (benzoate C-3), 135.4 (ArC-2), 133.6 (ArC-3), 132.4 (PhC-quart.), 131.5 (ArC-4), 129.4 (PhC-ortho), 129.0 (benzoate C-5), 127.3 (PhC-meta), 125.9 (PhC-para and benzoate C-1), 125.4 (ArC-5 and ArC-1), 124.9 (benzoate C-6), 124.0 (benzoate C-4), 120.6 (benzoate C-2), 113.5 (C-4), (quartet for CF_3 not observed); LC-MS (ESI): calc. for $\text{C}_{24}\text{H}_{15}\text{ClF}_3\text{N}_2\text{O}_4$ $[\text{M}+\text{H}]^+$: 487.06, observed: 487.25, LC R_t : 7.10 min. HRMS (ESI): calc. for $\text{C}_{24}\text{H}_{15}\text{ClF}_3\text{N}_2\text{O}_4$ $[\text{M}+\text{H}]^+$: 487.0672 observed: 487.0667.

4.3.20. 4-{3-[2-Chloro-6-(trifluoromethyl)phenyl]-5-phenyl-1,2-oxazole-4-amido}-2-fluorobenzoic acid (17). According to the General Procedure for amide coupling, carboxylic acid **11b** (0.200 g, 0.540 mmol) was coupled with methyl-4-amino-2-fluorobenzoate. The crude product was purified by flash column chromatography, eluting with a gradient of 20% - 25% EtOAc in n-heptane, to furnish the amide (0.075 g, 27%). The intermediate product (0.063 g, 0.120 mmol) was subject to ester hydrolysis according to the General Procedure for ester hydrolysis and purified by trituration with Et_2O to furnish **17** (0.053 g, 87%) as a colourless solid. $R_f = 0.27$ (1:1 n-heptane-EtOAc); ^1H -NMR (400

MHz, DMSO-d₆): δ (ppm) 13.05 (1 H, br. s, CO₂H), 10.94 (1 H, s, CONH), 7.99 (1 H, d, J = 8.2, ArH-3 or ArH-5), 7.94 (1 H, d, J = 7.9, ArH-3 or ArH-5), 7.87-7.78 (4 H, m, PhH-ortho, ArH-4, benzoate H-6), 7.62-7.59 (3 H, m, PhH-meta, PhH-para), 7.51 (1 H, d, J = 13.1, benzoate H-3), 7.28 (1 H, d, J = 8.7, benzoate H-5); ¹³C-NMR (100 MHz, DMSO-d₆): δ (ppm) 167.3 (C-5), 164.5 (CO₂H), 161.5 (d, J = 256.0, benzoate C-2), 159.1 (CO₂NH), 158.7 (C-3), 143.6 (d, J = 11.4, benzoate C-4), 135.4 (ArC-2), 133.7 (ArC-3), 132.8 (benzoate C-6), 132.4 (PhC-quart.), 131.7 (ArC-4), 130.4 (q, J = 30.6, ArC-6), 129.4 (PhC-ortho), 127.4 (PhC-meta), 125.7 (PhC-para), 125.4 (ArC-5), 125.1 (ArC-1), 122.9 (q, J = 274.6, CF₃), 115.0 (benzoate C-5), 114.2 (d, J = 10.1, benzoate C-1), 113.1 (C-4), 107.2 (d, J = 27.5, benzoate C-3); LC-MS (ESI): calc. for C₂₄H₁₄ClF₄N₂O₄ [M+H]⁺: 505.05, observed: 505.25, LC R_t: 7.10 min. HRMS (ESI): calc. for C₂₄H₁₄ClF₄N₂O₄ [M+H]⁺: 505.0578 observed: 505.0569.

4.3.21. 4-[(3-[2-chloro-6-(trifluoromethyl)phenyl]-5-phenyl-1,2-oxazol-4-yl)formamido)methyl]benzoic acid (**18**). According to the General Procedure for amide coupling, carboxylic acid **11b** (0.200 g, 0.540 mmol) was coupled with methyl-4-aminomethyl benzoate. The crude product was purified by flash column chromatography,

eluting with 15% EtOAc in cyclo-hexane, to furnish the amide (0.173 g, 62%). The intermediate product (0.106 g, 0.200 mmol) was subject to ester hydrolysis according to the General Procedure for ester hydrolysis and purified by trituration with Et₂O to furnish **18** (0.096 g, 96%) as a colourless solid. *R_f* = 0.51 (9:1 CH₂Cl₂-MeOH); ¹H-NMR (400 MHz, MeOD): δ (ppm) 7.91 (2 H, d, *J* = 8.3, benzoate H-2), 7.84 (1 H, d, *J* = 7.7, ArH-3 or ArH-5), 7.83 (1 H, d, *J* = 8.3, ArH-3 or ArH-5), 7.78-7.76 (2 H, m, PhH-ortho), 7.72 (1 H, app. t, *J* = 8.0, ArH-4), 7.57-7.53 (1 H, m, PhH-para), 7.49-7.45 (2 H, m, PhH-meta), 7.24 (2 H, d, *J* = 8.3, benzoate H-3), 4.42 (1 H, d, *J* = 15.2, benzylic CH_a), 4.40 (1 H, d, *J* = 15.2, benzylic CH_b); ¹³C-NMR (100 MHz, DMSO-d₆): δ (ppm) 167.2 (C-5), 166.6 (CO₂H), 160.0 (CO₂NH), 158.4 (C-3), 143.6 (benzoate C-4), 135.6 (ArC-2), 133.6 (ArC-3), 132.3 (PhC-quart.), 131.3 (ArC-4), 130.6 (q, *J* = 31.6, ArC-6), 129.5 (benzoate C-1), 129.2 (benzoate C-2 and PhC-ortho), 127.5 (PhC-meta), 127.4 (PhC-para), 125.9 (ArC-5), 125.4 (ArC-1), 122.9 (q, *J* = 274.1, CF₃), 118.8 (benzoate C-3), 113.6 (C-4), 42.4 (benzylic CH₂); LC-MS (ESI): calc. for C₂₅H₁₇ClF₃N₂O₄ [M+H]⁺: 501.08, observed: 501.25, LC R_t: 6.67 min. HRMS (ESI): calc. for C₂₅H₁₇ClF₃N₂O₄ [M+H]⁺: 501.0829 observed: 501.0818.

4.3.22. 4-[(3-[2-Chloro-6-(trifluoromethyl)phenyl]-5-phenyl-1,2-oxazol-4-yl)methyl]amino] benzoic acid (19). Ethyl-4-aminobenzoate (86 mg, 0.52 mmol, 1.0 eq) and AcOH (0.5 mL) were added to a solution of aldehyde **12** (0.183 g, 0.520 mmol, 1.0 eq) in EtOH (10.0 mL). The reaction mixture was heated at reflux for 4h after which time it was cooled to room temperature and NaCNBH₃ (65.3 mg, 1.04 mmol, 2.0 eq) was added. The reaction mixture was then heated at reflux for a further 12 h then concentrated *in vacuo*, diluted with EtOAc (10 ml) and washed with saturated aqueous NaHCO₃ (20 mL), water (20 mL) and brine (20 mL). The combined organic phase was dried (MgSO₄), filtered and concentrated *in vacuo*. The crude product was purified by flash column chromatography, eluting with 17% EtOAc in n-heptane, to furnish the ester (81.4 mg, 31%). The intermediate product (0.049 g, 0.098 mmol) was subject to ester hydrolysis according to the General Procedure for ester hydrolysis and purified by trituration with Et₂O to furnish **19** (0.046 g, 99%) as a colourless solid. *R_f* = baseline (4:1 cyclo-hexane-EtOAc); ¹H-NMR (400 MHz, DMSO-d₆): δ (ppm) 12.03 (1 H, br. s, CO₂H), 7.92-7.85 (4 H, m, ArH-3, ArH-5, PhH-ortho), 7.73 (1 H, app. t, *J* = 8.0, ArH-4), 7.64-7.58 (3 H, m, PhH-ortho and PhH-meta), 7.53 (2 H, d, *J* = 8.8, benzoate C-2), 6.48 (1 H, t, *J* = 5.3 CH₂NH), 6.37 (2 H, d, *J* = 8.8, benzoate H-3), 4.21 (1 H, dd, *J* = 14.7, 5.3, CH_aNH), 4.12 (1 H, dd, *J* = 14.7, 5.3, CH_bNH); ¹³C-NMR (100 MHz, DMSO-d₆): δ (ppm) 167.4 (C-5), 166.4 (CO₂H), 159.6 (C-3), 151.6 (benzoate C-4), 135.5 (ArC-2), 133.7 (ArC-3), 132.2 (PhC-quart.), 130.8 (benzoate C-2), 130.7 (ArC-4), 130.6 (q, *J* = 30.4, ArC-6), 129.3 (PhC-ortho), 127.2 (PhC-meta), 126.6 (PhC-para), 125.6 125.4 (ArC-5), 125.4 (q, *J* = 5.0, ArC-1), 122.9 (q, *J* = 274.6, CF₃), 117.6 (benzoate C-1), 113.1 (C-4), 110.7 (benzoate C-3), 35.7 (CH₂NH); LC-MS (ESI): calc. for C₂₄H₁₇ClF₃N₂O₃ [M+H]⁺: 473.08,

observed 473.00, LC R_t : 7.35 min. HRMS (ESI): calc. for $C_{24}H_{17}ClF_3N_2O_3$ $[M+H]^+$: 473.0880

observed: 473.0862.

4.3.23. 4-({3-[2-Chloro-6-(trifluoromethyl)phenyl]-5-phenyl-1,2-oxazol-4-yl}carbamoyl)

benzoic acid (20). According to the General Procedure for amide coupling, mono-methyl terephthalate (23.0 mg, 0.120 mmol) was coupled with amine **13** (43.0 mg, 0.120 mmol).

The crude product was purified by flash column chromatography, eluting with 25% EtOAc in c-hexane, to furnish the amide (46.0 mg, 76%). The intermediate product (35.0 mg,

0.070 mmol) was subject to ester hydrolysis according to the General Procedure for ester hydrolysis and purified by trituration with Et_2O to furnish **20** (22.6 mg, 66%) as a colourless

solid. R_f = 0.56 (9:1 CH_2Cl_2 -MeOH); 1H -NMR (400 MHz, $DMSO-d_6$): δ (ppm) 13.21 (1 H, br. s, CO_2H), 10.39 (1 H, s, $NHCO$), 8.01 (2 H, d, J =8.4, benzoate C-3), 7.94-7.86 (6 H,

m, benzoate C-2, ArH-3 and ArH-5, phenyl H-ortho), 7.75 (1 H, app. t, J = 8.0, ArH-4), 7.59-7.51 (3 H, m, phenyl H-meta and phenyl H-para); ^{13}C -NMR (100 MHz, $CDCl_3$): δ

(ppm) 166.7 (C-5), 165.2 (CO_2H), 161.7 (CO_2NH), 157.8 (C-3), 137.1 (benzoate C-4), 135.3 (PhC-quart), 133.8 (benzoate C-1), 133.6 (ArC-3), 132.2 (ArC-2), 130.9 (q, J =30.9,

ArC-6), 130.6 (benzoate C-4), 129.3 (benzoate C-2), 129.2 (PhC-ortho), 127.9 (PhC-

meta), 126.4 (PhC-para), 125.9 (benzoate C-3), 125.7 (q, $J = 5.0$, ArC-5), 125.1 (ArC-1),
122.9 (q, $J = 274.7$, CF_3), 114.5 (C-4); LC-MS (ESI): calc. for $\text{C}_{24}\text{H}_{15}\text{ClF}_3\text{N}_2\text{O}_4$ $[\text{M}+\text{H}]^+$:
487.06, observed 487.17, LC R_t : 6.73 min. HRMS (ESI): calc. for $\text{C}_{24}\text{H}_{15}\text{ClF}_3\text{N}_2\text{O}_4$ $[\text{M}+\text{H}]^+$:
487.0672 observed: 487.0677.

4.3.24. 4-[(3-[2-Chloro-6-(trifluoromethyl)phenyl]-5-phenyl-1,2-oxazol-4-yl)amino) methyl] benzoic acid (21). Methyl-4-formyl benzoate (93.0 mg, 0.570 mmol, 1.0 eq) and AcOH (0.5 mL) were added to a solution of amine **13** (0.201 g, 0.590 mmol, 1.05 eq) in MeOH (10.0 mL). The reaction mixture was heated at reflux for 18 h after which time it was cooled to room temperature and NaCNBH_3 (74.0 mg, 1.18 mmol, 2.0 eq) was added. The reaction mixture was heated at reflux for a further 18 h then concentrated *in vacuo*, diluted with EtOAc (10 mL) and washed with saturated aqueous NaHCO_3 (20 mL), water (20 mL) and brine (20 mL). The combined organic phase was dried (MgSO_4), filtered and concentrated *in vacuo*. The crude product was purified by flash column chromatography, eluting with 17% EtOAc in n-heptane, to furnish the ester (0.120 g, 43%). The intermediate product (0.106 g, 0.220 mmol) was subject to ester hydrolysis according to the General Procedure for ester hydrolysis and purified by trituration with Et_2O to furnish

21 (0.094 g, 98%) as a colourless solid. R_f = baseline (1:1 cyclo-hexane-EtOAc); $^1\text{H-NMR}$ (400 MHz, DMSO-d_6): δ (ppm) 12.82 (1 H, br. s, CO_2H), 7.95 (1 H, d, $J = 8.1$, ArH-3), 7.88 (1 H, d, $J = 8.1$, ArH-5), 7.84 (2 H, d, $J = 7.3$, PhH-ortho), 7.80-7.78 (1 H, m, ArH-4), 7.75 (2 H, d, $J = 8.1$, benzoate H-2), 7.53-7.50 (2 H, m, PhH-meta), 7.47-7.43 (1 H, m, PhH-para), 7.15 (2 H, d, $J = 8.1$, benzoate H-3), 5.11 (1 H, app. t, $J = 6.0$, NHCH_2), 4.00 (1 H, dd, $J = 15.5, 6.0$, NHCH_a), 3.94 (1 H, dd, $J = 15.5, 6.0$, NHCH_b); $^{13}\text{C-NMR}$ (100 MHz, DMSO-d_6): δ (ppm) 167.2 (C-5), 155.3 (CO_2H), 154.3 (C-3), 145.0 (benzoate C-4), 136.0 (ArC-2), 133.6 (ArC-3), 132.2 (PhC-quart.), 131.1 (q, $J = 30.5$, ArC-6), 129.22 (benzoate C-1), 129.17 (ArC-4), 129.0 (PhC-ortho), 128.9 (benzoate C-2), 127.6 (PhC-para), 127.1 (PhC-meta), 126.0 (ArC-5), 125.9 (C-4), 125.7 (benzoate C-3), 125.4 (q, $J = 5.0$, ArC-1), 122.9 (q, $J = 274.6$, CF_3), 49.8 (CH_2NH); LC-MS (ESI): calc. for $\text{C}_{24}\text{H}_{17}\text{ClF}_3\text{N}_2\text{O}_3$ $[\text{M}+\text{H}]^+$: 473.08, observed 473.17, LC R_t : 7.48 min. HRMS (ESI): calc. for $\text{C}_{24}\text{H}_{17}\text{ClF}_3\text{N}_2\text{O}_3$ $[\text{M}+\text{H}]^+$: 473.0880 observed: 473.0883.

4.3.25. 4-({3-[2-Chloro-6-(trifluoromethyl)phenyl]-5-phenyl-1,2-oxazol-4-yl}sulfamoyl)benzoic acid (**22**). Methyl-4-(chlorosulfonyl)benzoate (0.464 g, 1.70 mmol, 3.0 eq) was added to a solution of amine **13** (0.192 g, 0.570 mmol, 1.0 eq) in pyridine (10.0 mL). The

reaction mixture was stirred at 60 °C for 24 h then cooled to room temperature and concentrated *in vacuo*. The mixture was suspended in EtOAc (20 mL) and washed with 1 M aqueous HCl (20 mL), saturated aqueous NaHCO₃ (20 mL), water (20 mL) and brine (20 mL). The organic phase was dried (MgSO₄), filtered and concentrated *in vacuo* to furnish the ester (0.260 g, 71%) that was used without further purification. The intermediate product (0.188 g, 0.350 mmol) was subject to ester hydrolysis according to the General Procedure for ester hydrolysis and purified by trituration with Et₂O to furnish **22** (0.079 g, 43%) as a yellow solid. *R*_f = baseline (1:1 cyclo-hexane-EtOAc); ¹H-NMR (400 MHz, DMSO-d₆): δ (ppm) 13.30 (1 H, br. s, CO₂H), 10.49 (1 H, br. s, N⁺SO₂), 7.87 (1 H, d, *J* = 8.0, ArC-3), 7.79 (1 H, d, *J* = 8.0, ArC-5), 7.75-7.68 (5 H, m, ArH-4, PhH-ortho, benzoate H-3), 7.51 (2 H, d, *J* = 8.2, benzoate H-2), 7.46-7.37 (3 H, m, PhH-meta and PhH-para); ¹³C-NMR (100 MHz, DMSO-d₆): δ (ppm) 165.9 (C-5), 164.8 (CO₂H), 159.2 (C-3), 143.6 (benzoate C-4), 135.4 (ArC-2), 134.2 (ArC-3), 133.5 (benzoate C-1), 132.3 (PhC-quart.), 130.9 (q, *J* = 30.9, ArC-6), 130.8 (ArC-4), 129.7 (benzoate C-2), 128.8 (PhC-ortho), 126.2 (benzoate C-3), 126.1 (PhC-meta), 125.5 (q, *J* = 5.0, ArC-1), 125.2 (PhC-para), 124.4 (ArC-5), 122.8 (q, *J* = 274.5, CF₃), 112.4 (C-4); LC-MS (ESI): calc. for

$C_{23}H_{15}ClF_3N_2O_5S$ $[M+H]^+$: 523.03, observed 523.00, LC R_t : 6.70 min. HRMS (ESI): calc. for $C_{23}H_{15}ClF_3N_2O_5S$ $[M+H]^+$: 523.0342 observed: 523.0333.

4.3.26. **4-[(3-[2-Chloro-6-(trifluoromethyl)phenyl]-5-(furan-2-yl)-1,2-oxazol-4-yl)methyl]amino]benzoic acid (23).** According to the General Procedure for reductive amination, aldehyde **39** (0.180 g, 0.520 mmol) was reacted with *tert*-butyl-4-amino benzoate (0.102 g, 0.520 mmol) in MeOH. The crude product was purified by column chromatography, eluting with a gradient of 5-20% EtOAc in n-heptane, to furnish the intermediate imine (0.136 g) that was immediately subjected to the reduction step performed in EtOH at 85 °C. The crude product was purified by column chromatography, eluting with a gradient of 10-20% EtOAc in n-heptane, to furnish the intermediate amine (0.065 g, 24%). This product was subject to *tert*-butyl ester deprotection according to the General Procedure for *tert*-Butyl ester deprotection. The crude product was purified by column chromatography, eluting with 1% MeOH in CH_2Cl_2 , to furnish the carboxylic acid **23** (0.040 g, 73%) as a colourless solid. R_f = 0.13 (99:1 CH_2Cl_2 -MeOH); 1H -NMR (400 MHz, MeOD): δ (ppm) 7.84 (1 H, d, J = 1.8, furanyl H-5), 7.75 (1 H, d, J = 8.1, Ar H-3 or ArH-5), 7.74 (1 H, d, J = 8.1, ArH-3 or ArH-5), 7.61 (1 H, app. t, J = 8.1, ArH-4), 7.61 (2

H, d, $J=8.8$, benzoate H-2), 7.12 (1 H, d, $J= 3.5$, furanyl H-3), 7.62 (1 H, dd, $J= 3.5, 1.8$, furanyl H-4), 6.34 (2 H, d, $J=8.8$, benzoate H-3), 4.46 (1 H, d, $J= 15.3$, CH_aNH), 4.36 (1 H, d, $J= 15.3$, CH_bNH); ^{13}C -NMR (100 MHz, $CDCl_3$): δ (ppm) 170.5 (C-5), 160.6 (CO_2H), 159.9 (C-3), 153.4 (furanyl C-2), 146.5 (furanyl C-5), 144.1 (benzoate C-4), 137.6 (ArC-2), 134.6 (ArC-3), 132.9 (q, $J= 32.5$, ArC-6), 132.7 (ArC-4), 132.4 (benzoate C-2), 127.3 (ArC-1), 126.3 (q, $J= 5.1$, ArC-5), 124.4 (q, $J= 273.8$, CF_3), 118.7 (benzoate C-1), 114.6 (C-4), 113.2 (furanyl C-4), 113.1 (furanyl C-3), 111.8 (benzoate C-3), 36.4 (CH_2NH); LC-MS (ESI): calc. for $C_{22}H_{15}ClF_3N_2O_4$ $[M+H]^+$: 463.06, observed: 462.92, LC R_t : 6.67 min; HRMS (ESI): calc. for $C_{22}H_{15}ClF_3N_2O_4$ $[M+H]^+$: 463.0672, observed: 463.0661.

4.3.27. 4-[(3-[2-Chloro-6-(trifluoromethyl)phenyl]-5-(thiophen-2-yl)-1,2-oxazol-4-yl)methyl]amino]benzoic acid (24). According to the General Procedure for reductive amination, aldehyde **40** (0.096 g, 0.270 mmol) was reacted with *tert*-butyl-4-amino benzoate (0.052 g, 0.27 mmol) in MeOH. The crude product was purified by column chromatography, eluting with a gradient of 5-10% EtOAc in n-heptane, to furnish the intermediate imine (0.125 g) that was immediately subjected to the reduction step performed in EtOH at 85 °C for 5 h. The crude product was purified by column

chromatography, eluting with a gradient of 3-10% EtOAc in n-heptane, to furnish the intermediate amine (24.0 mg, 17%). This product was subject to *tert*-butyl ester deprotection according to the General Procedure for *tert*-Butyl ester deprotection. The crude product was purified by column chromatography, eluting with 3% MeOH in CH₂Cl₂, to furnish the carboxylic acid **24** (12.0 mg, 56%) as a pale yellow solid. *R_f* = 0.13 (98:2 CH₂Cl₂-MeOH); ¹H-NMR (400 MHz, DMSO-d₆): δ (ppm) 12.02 (1 H, br. s, CO₂H), 7.96 (1 H, dd, *J* = 5.1, 1.1, thiophenyl H-5), 7.93 (1 H, d, *J* = 8.0, ArH-3 or ArH-5), 7.87 (1 H, d, *J* = 8.0, ArH-3 or ArH-5), 7.77-7.73 (2 H, m, ArH-4, thiophenyl H-3), 7.55 (2 H, d, *J* = 8.8, benzoate H-2), 7.33 (1 H, dd, *J* = 5.1, 3.7, thiophenyl H-4), 6.48 (1 H, app. t, *J* = 5.0, CH₂NH), 6.42 (2 H, d, *J* = 8.8, benzoate H-3), 4.20 (1 H, dd, *J* = 14.8, 5.0, CH_aNH), 4.13 (1 H, dd, *J* = 14.8, 5.0, CH_bNH); ¹³C-NMR (100 MHz, DMSO-d₆): δ (ppm) 167.4 (C-5), 162.0 (CO₂H), 159.5 (C-3), 151.6 (benzoate C-4), 135.5 (ArC-2), 133.8 (ArC-3), 132.3 (ArC-4), 130.8 (benzoate C-2), 130.6 (q, *J* = 30.7, ArC-6), 130.6 (thiophenyl C-5), 128.8 (thiophenyl C-3), 128.7 (thiophenyl C-4), 127.2 (thiophenyl C-2), 125.5 (q, *J* = 4.9, ArC-5), 125.3 (ArC-1), 122.8 (q, *J* = 274.5, CF₃), 117.6 (benzoate C-1), 112.0 (C-4), 110.8 (benzoate C-3), 35.6 (CH₂NH); LC-MS (ESI): calc. for C₂₂H₁₅ClF₃N₂O₃S [M+H]⁺: 479.04,

observed: 479.00, LC R_t : 7.23 min. HRMS (ESI): calc. for $C_{22}H_{15}ClF_3N_2O_3S$ $[M+H]^+$:
479.0444, observed: 479.0429.

4.3.28. 4-[(3-[2-Chloro-6-(trifluoromethyl)phenyl]-5-(1H-pyrrol-3-yl)-1,2-oxazol-4-yl)methyl]amino]benzoic acid (25). According to the General Procedure for reductive amination, aldehyde **41** (0.060 g, 0.176 mmol) was reacted with methyl-4-amino benzoate (0.032 g, 0.211 mmol) in MeOH. The crude product was purified by column chromatography, eluting with 25% EtOAc in *n*-heptane, to furnish the intermediate imine (0.034 mg) that was immediately subjected to the reduction step performed in MeOH at reflux for 2 h. The crude product was purified by column chromatography, eluting with a gradient of 20% EtOAc in *n*-heptane, to furnish the intermediate amine (16.3 mg, 19%). This product was subject to ester hydrolysis according to the General Procedure for tert-Butyl ester deprotection. The crude product was purified by column chromatography, eluting with 1.5% MeOH in CH_2Cl_2 , to furnish the carboxylic acid **25** (5.40 mg, 57%) as a colourless solid. R_f = 0.10 (96:4 CH_2Cl_2 -MeOH); 1H -NMR (400 MHz, DMSO- d_6): δ (ppm) 11.99 (1 H, br. s, CO_2H), 11.52 (1 H, s, pyrrole- NH), 7.91 (1 H, d, J = 8.1, ArH-3 or ArH-5), 7.85 (1 H, d, J = 7.9, ArH-3 or ArH-5), 7.72 (1 H, app. t, J = 8.0, ArH-4), 7.54 (2 H, d,

$J = 8.4$, benzoate C-2), 7.39 (1 H, m, pyrrole H-2), 6.98 (1 H, app. q, $J = 2.4$, pyrrole H-5), 6.55 (1 H, d, $J = 2.4$, pyrrole H-4), 6.42 (2 H, d, $J = 8.4$, benzoate H-3), 6.34 (1 H, app. t, $J = 5.0$, CH_2NH), 4.08 (1 H, dd, $J = 14.5, 5.0$, CH_aNH), 4.00 (1 H, dd, $J = 14.5, 5.0$, CH_bNH); ^{13}C -NMR (100 MHz, DMSO-d_6): δ (ppm) 167.9 (C-5), 165.7 (CO_2H), 159.2 (C-3), 152.3 (benzoate C-4), 136.0 (ArC-2), 134.1 (ArC-3), 132.4 (ArC-4), 131.3 (benzoate C-2), 130.9 (q, $J = 30.4$, ArC-6), 126.8 (ArC-1), 125.8 (q, $J = 5.0$, ArC-5), 122.0 (q, $J = 274.3$, CF_3), 120.5 (pyrrole C-5), 119.2 (pyrrole C-2), 117.8 (benzoate C-1), 111.2 (benzoate C-3), 110.5 (C-4), 109.2 (pyrrole C-3), 106.7 (pyrrole C-4), 36.2 (CH_2NH); LC-MS (ESI): calc. for $\text{C}_{22}\text{H}_{16}\text{ClF}_3\text{N}_3\text{O}_3$ $[\text{M}+\text{H}]^+$: 462.08, observed: 462.00, LC R_t : 6.20 min. HRMS (ESI): calc. for $\text{C}_{22}\text{H}_{16}\text{ClF}_3\text{N}_3\text{O}_3$ $[\text{M}+\text{H}]^+$: 462.0832, observed: 462.0834.

4.3.29. 4-[(3-[2-Chloro-6-(trifluoromethyl)phenyl]-5-(naphthalen-1-yl)-1,2-oxazol-4-yl)methyl]amino]benzoic acid (26). According to the General Procedure for reductive amination, aldehyde **42** (0.034 g, 0.0850 mmol) was reacted with *tert*-butyl-4-amino benzoate (0.016 g, 0.085 mmol) in MeOH. The crude product was purified by column chromatography, eluting with a gradient of 2-10% EtOAc in *n*-heptane, to furnish the intermediate imine (0.010 g) that was immediately subjected to the reduction step

performed in EtOH at 85 °C for 5 h. The crude product was purified by column chromatography, eluting with 20% EtOAc in n-heptane, to furnish the intermediate amine (8.00 mg, 16%). This product was subject to *tert*-butyl ester deprotection according to the General Procedure for *tert*-Butyl ester deprotection. The crude product was purified by column chromatography, eluting with 3% MeOH in CH₂Cl₂, to furnish the carboxylic acid **26** (3.00 mg, 48%) as a colourless solid. *R*_f = 0.16 (96:4 CH₂Cl₂-MeOH); ¹H-NMR (400 MHz, DMSO-d₆): δ (ppm) 11.93 (1 H, br. s, CO₂H), 8.23 (1 H, d, *J* = 8.3, naphthyl-H), 8.12 (1 H, d, *J* = 7.5, naphthyl-H), 7.94 (1 H, d, *J* = 8.0, ArH-3 or ArH-5), 7.88 (1 H, d, *J* = 8.0, ArH-3 or ArH-5), 7.84 (1 H, d, *J* = 7.0, naphthyl-H), 7.76-7.66 (5 H, m, ArH-4, naphthyl-H), 7.31 (2 H, d, *J* = 8.3, benzoate C-2), 6.36 (1 H, app. t, *J* = 5.8, CH₂NH), 6.08 (2 H, d, *J* = 8.3, benzoate C-3), 4.08 (1 H, dd, *J* = 15.8, 5.8, CH_aNH), 4.01 (1 H, dd, *J* = 15.8, 5.8, CH_bNH); ¹³C-NMR (100 MHz, DMSO-d₆): δ (ppm) 167.3 (C-5), 166.9 (CO₂H), 158.8 (C-3), 151.3 (benzoate C-4), 135.4 (ArC-2), 133.7 (ArC-3), 133.3 (naphthyl-C), 132.1 (ArC-4), 131.4 (naphthyl-C), 130.9 (naphthyl-C), 130.5 (q, *J* = 31.1, ArC-6), 130.5 (benzoate C-2), 129.3 (naphthyl-C), 128.7 (naphthyl-C), 127.8 (naphthyl-C), 126.8 (naphthyl-C), 125.8 (ArC-1), 125.5 (q, *J* = 4.0, ArC-5), 125.4 (naphthyl-C), 124.3

(naphthyl-C), 123.5 (naphthyl-C), 123.0 (q, $J = 274.3$, CF_3), 117.2 (benzoate C-1), 116.3 (C-4), 110.4 (benzoate C-3), 35.3 (CH_2NH); LC-MS (ESI): calc. for $\text{C}_{28}\text{H}_{19}\text{ClF}_3\text{N}_2\text{O}_3$ $[\text{M}+\text{H}]^+$: 523.10, observed: 522.92, LC R_t : 7.68 min. HRMS (ESI): calc. for $\text{C}_{28}\text{H}_{19}\text{ClF}_3\text{N}_2\text{O}_3$ $[\text{M}+\text{H}]^+$: 523.1036, observed: 523.1046.

4.3.30. 4-[(3-[2-Chloro-6-(trifluoromethyl)phenyl]-5-(3-hydroxyphenyl)-1,2-oxazol-4-yl)methyl]amino]benzoic acid (27). According to the General Procedure for reductive amination, aldehyde **43** (0.123 g, 0.255 mmol) was reacted with methyl-4-amino benzoate (0.038 g, 0.255 mmol) in MeOH. The crude product was purified by column chromatography, eluting with a gradient of 2-12% EtOAc in n-heptane, to furnish the intermediate imine (0.053 g) that was immediately subjected to the reduction step performed in MeOH at reflux for 3.5 h. This step occurred with concomitant loss of the silyl protecting group. The crude product was purified by column chromatography, eluting with a gradient of 15-35% EtOAc in n-heptane, to furnish the intermediate amine (21.0 mg, 16%). This product was subject to ester hydrolysis according to the General Procedure for tert-Butyl ester deprotection. The crude product was purified by column chromatography, eluting with 3% MeOH in CH_2Cl_2 , to furnish the carboxylic acid **27** (17.4

mg, 99%) as a colourless solid. $R_f = 0.10$ (96:4 CH_2Cl_2 -MeOH); $^1\text{H-NMR}$ (400 MHz, DMSO-d_6): δ (ppm) 7.90 (1 H, d, $J = 8.1$, ArH-3 or ArH-5), 7.85 (1 H, d, $J = 8.0$, ArH-3 or ArH-5), 7.72 (1 H, app. t, $J = 8.0$, ArH-4), 7.52 (2 H, d, $J = 8.8$, benzoate H-2), 7.40 (1 H, app. t, $J = 8.0$, phenol H-5), 1.30-7.26 (2 H, m, phenol H-2 and phenol H-4), 6.99 (1 H, dd, $J = 8.0$, 1.5, phenol H-6), 6.42 (1 H, t, $J = 5.0$, CH_2NH), 6.36 (2 H, d, $J = 8.8$, benzoate H-3), 4.17 (1 H, dd, $J = 14.6$, 5.0, CH_aNH), 4.09 (1 H, dd, $J = 14.6$, 5.0, CH_bNH); $^{13}\text{C-NMR}$ (100 MHz, DMSO-d_6): δ (ppm) 167.4 (C-5), 166.4 (CO_2H), 159.6 (C-3), 157.9 (phenol C-3), 151.6 (benzoate C-4), 135.5 (ArC-2), 133.7 (ArC-3), 132.2 (ArC-4), 130.8 (benzoate C-2), 130.5 (q, $J = 30.7$, ArC-6), 130.5 (phenol C-1), 127.7 (phenol C-5), 125.7 (ArC-1), 125.4 (q, $J = 4.0$, ArC-5), 122.8 (q, $J = 274.3$, CF_3), 117.8 (phenol C-6), 117.6 (benzoate C-1), 113.6 (phenol C-2), 112.9 (C-4), 110.7 (benzoate C-3), 35.7 (CH_2NH); LC-MS (ESI): calc. for $\text{C}_{24}\text{H}_{17}\text{ClF}_3\text{N}_2\text{O}_4$ $[\text{M}+\text{H}]^+$: 489.08, observed: 489.00, LC R_t : 6.30 min. HRMS (ESI): calc. for $\text{C}_{24}\text{H}_{17}\text{ClF}_3\text{N}_2\text{O}_4$ $[\text{M}+\text{H}]^+$: 489.0829, observed: 489.0823.

4.3.31. Methyl 5-bromo-3-[2-chloro-6-(trifluoromethyl)phenyl]-1,2-oxazole-4-carboxylate (30a). Methyl 3-bromopropiolate (prepared according to Ref. 44, 2.04 g, 12.5 mmol, 1.0 eq) was added to a solution of nitrile oxide **33** (2.75 g, 12.5 mmol, 1.0 eq) in

THF (25.0 mL) and the reaction mixture was heated at reflux for 4 h. The reaction mixture was concentrated *in vacuo* to give a crude product as a 7:3 mixture of regioisomers. Purification by recrystallization from hot n-heptane furnished bromide **30a** (2.05 g, 43%) as a colourless solid (97:3 mixture of regioisomers – see Supporting Information). R_f = 0.20 (7:3 n-heptane-EtOAc); $^1\text{H-NMR}$ (400 MHz, CDCl_3): δ (ppm) 7.73 (1 H, d, J = 8.6, ArH-3 or ArH-5), 7.71 (1 H, d, J = 8.9, ArH-3 or ArH-5), 7.58 (1 H, app. t. J = 8.0, ArH-3), 3.70 (3 H, s, CO_2CH_3); $^{13}\text{C-NMR}$ (100 MHz, CDCl_3): δ (ppm) 160.0 (C-5), 159.7 (CO_2Me), 148.0 (C-3), 136.3 (ArC-2), 133.0 (ArC-3), 131.7 (q, J = 31.7, ArC-6), 131.3 (ArC-4), 126.0 (ArC-1), 124.8 (q, J = 5.0, ArC-5), 122.9 (q, J = 274.4, CF_3), 113.2 (C-4), 52.3 (CO_2CH_3); LC-MS (ESI): calc. for $\text{C}_{12}\text{H}_7\text{BrClF}_3\text{NO}_3$ $[\text{M}+\text{H}]^+$: 383.92, observed 386.00, LC R_t : 7.12 min.

4.3.32. [2-Chloro-6-(trifluoromethyl)phenyl]formonitrile oxide (33). NEt_3 (5.80 mL, 41.5 mmol, 1.2 eq) was added dropwise to a solution of imidoyl chloride **9a** (8.90 g, 34.6 mmol, 1.0 eq) in THF (110 mL). A white precipitate formed immediately. The resulting suspension was stirred vigorously at room temperature for 30 min and then filtered through a pad of SiO_2 that was subsequently washed with THF (250 mL). The solution

was concentrated *in vacuo* to furnish **33** (8.25 g, 99%) as a colourless solid which was used immediately. R_f = 0.33 (9:1 c-hexane-EtOAc); $^1\text{H-NMR}$ (400 MHz, CDCl_3): δ (ppm) 7.70 (1 H, d, J = 8.2, H-3 or H-5), 7.67 (1 H, d, J = 8.2, H-3 or H-5), 7.54 (1 H, app. t, J = 8.2, H-4).

4.3.33. Methyl 3-[2-chloro-6-(trifluoromethyl)phenyl]-5-(furan-2-yl)-1,2-oxazole-4-carboxylate (34). According to the General Procedure for Suzuki coupling, bromide **30a** (0.150 g, 0.390 mmol) was coupled to furan-2-boronic acid pinacol ester (0.114 g, 0.585 mmol). The crude product was purified by flash column chromatography, eluting with a gradient of 10-50% EtOAc in n-heptane, to furnish **34** (0.088 g, 58%) as a colourless solid. R_f = 0.19 (85:15 n-heptane-EtOAc); $^1\text{H-NMR}$ (400 MHz, CDCl_3): δ (ppm) 7.82 (1 H, dd, J = 3.6, 0.7, furanyl H-5), 7.73 (1 H, d, J = 8.0, Ar H-3 or ArH-5), 7.72 (1 H, dd, J = 1.8, 0.7, furanyl H-3), 7.70 (1 H, d, J = 8.0, Ar H-3 or ArH-5), 7.56 (1 H, app. t, J = 8.0, ArH-4), 6.66 (1 H, dd, J = 3.6, 1.8, furanyl H-4), 3.62 (3 H, s, CO_2CH_3); $^{13}\text{C-NMR}$ (100 MHz, CDCl_3): δ (ppm) 163.4 (C-5), 160.9 (CO_2CH_3), 158.7 (C-3), 146.3 (furanyl C-3), 141.6 (furanyl C-2), 136.3 (ArC-2), 132.8 (ArC-3 and ArC-4), 131.6 (q, J = 31.3, ArC-6), 130.8 (ArC-4), 127.1 (ArC-1), 124.7 (q, J = 5.0, ArC-5), 123.0 (q, J = 274.5, CF_3), 118.3

(furanyl C-5), 112.6 (furanyl C-4), 107.3 (C-4), 51.9 (CO₂CH₃); LC-MS (ESI): calc. for C₁₆H₁₀ClF₃NO₄ [M+H]⁺: 371.02, observed: 372.08, LC R_t: 7.77 min.

4.3.34. Methyl 3-[2-chloro-6-(trifluoromethyl)phenyl]-5-(thiophen-2-yl)-1,2-oxazole-4-carboxylate (35). According to the General Procedure for Suzuki coupling, bromide **30a** (0.250 g, 0.650 mmol) was coupled to thiophene-2-boronic acid pinacol ester (0.273 g, 1.30 mmol). The crude product was purified by flash column chromatography, eluting with a gradient of 5% - 20% EtOAc in n-heptane, to furnish **35** (0.136 g, 54%) as a colourless solid. *R_f* = 0.32 (4:1 n-heptane-EtOAc); ¹H-NMR (400 MHz, CDCl₃): δ (ppm) 8.29 (1 H, dd, *J* = 3.9, 1.2, thiophenyl H-5), 7.75-7.69 (3 H, m, ArH-3, ArH-5, thiophenyl H-3), 7.57 (1 H, app. t, *J* = 8.0, ArH-4), 7.24 (1 H, dd, *J* = 5.1, 3.9, thiophenyl H-4), 3.64 (3 H, s, CO₂CH₃); ¹³C-NMR (100 MHz, CDCl₃): δ (ppm) 167.9 (C-5), 161.4 (CO₂CH₃), 159.2 (C-3), 136.3 (ArC-2), 132.8 (thiophenyl C-5), 132.7 (ArC-4), 132.2 (ArC-3 and thiophenyl C-3), 131.7 (q, *J* = 31.4, ArC-6), 130.8 (ArH-4), 128.0 (thiophenyl C-4), 127.4 (thiophenyl C-2), 127.3 (ArC-1), 124.7 (q, *J* = 5.0, ArC-5), 123.0 (q, *J* = 274.5, CF₃), 107.2 (C-4), 51.9 (CO₂CH₃); LC-MS (ESI): calc. for C₁₆H₁₀ClF₃NO₃S [M+H]⁺: 387.99, observed: 388.25, LC R_t: 7.62 min.

4.3.35. Methyl 5-{1-[(tert-butoxy)carbonyl]-1H-pyrrol-3-yl}-3-[2-chloro-6-(trifluoromethyl)phenyl]-1,2-oxazole-4-carboxylate (**36**). According to the General Procedure for Suzuki coupling, bromide **30a** (0.250 g, 0.650 mmol) was coupled to tert-butyl 3-(4,4,5,5-tetramethyl-1,3,2-dioxaborolan-2-yl)-1H-pyrrole-1-carboxylate (0.381 g, 1.30 mmol). The crude product was purified by flash column chromatography, eluting with a gradient of 5% - 20% EtOAc in n-heptane, to furnish **36** (0.119 g, 39%) as a colourless oil. R_f = 0.30 (4:1 n-heptane-EtOAc); $^1\text{H-NMR}$ (400 MHz, CDCl_3): δ (ppm) 8.45 (1 H, app. t, J = 2.0, pyrrole H-2), 7.72-7.67 (2 H, m, ArH-3 and ArH-5), 7.54 (1 H, app. t, J = 7.9, ArH-4), 7.35 (1 H, dd, J = 3.4, 2.0, pyrrole H-5), 6.98 (dd, J = 3.4, 2.0, pyrrole H-4), 3.61 (3 H, s, CO_2CH_3), 1.63 (9 H, s, $\text{C}(\text{CH}_3)_3$); $^{13}\text{C-NMR}$ (100 MHz, CDCl_3): δ (ppm) 168.9 (C-5), 161.6 (CO_2CH_3), 159.0 (C-3), 148.2 (NCO_2), 136.3 (ArC-2), 132.8 (ArC-3), 131.6 (q, J = 31.3, ArC-6), 130.6 (ArC-4), 127.7 (ArC-1), 124.7 (q, J = 5.0, ArC-5), 124.1 (pyrrole C-2), 123.0 (q, J = 274.4, CF_3), 121.0 (pyrrole C-5), 113.8 (pyrrole C-3), 111.5 (pyrrole C-4), 107.2 (C-4), 85.2 ($\text{C}(\text{CH}_3)_3$), 51.7 (CO_2CH_3), 28.0 ($\text{C}(\text{CH}_3)_3$); LC-MS (ESI): calc. for $\text{C}_{21}\text{H}_{19}\text{ClF}_3\text{N}_2\text{O}_5$ $[\text{M}+\text{H}]^+$: 471.09, observed: 471.17, LC R_t : 8.55 min.

4.3.36. Methyl 3-[2-chloro-6-(trifluoromethyl)phenyl]-5-(naphthalen-1-yl)-1,2-oxazole-4-carboxylate (37). According to the General Procedure for Suzuki coupling, bromide **30a** (0.150 g, 0.390 mmol) was coupled to naphthalene-1-boronic acid pinacol ester (0.198 g, 0.780 mmol). The crude product was purified by flash column chromatography, eluting with a gradient of 10% - 20% EtOAc in n-heptane, to furnish **37** (0.059 g, 35%) as a colourless oil. $R_f = 0.43$ (4:1 n-heptane-EtOAc); $^1\text{H-NMR}$ (400 MHz, CDCl_3): δ (ppm) 8.07 (1 H, d, $J = 8.3$, naphthyl-H), 7.97-7.94 (1 H, m, naphthyl-H), 7.81-7.75 (3 H, m, naphthyl-H), 7.73-7.71 (1 H, m, ArH-3 or ArH-5), 7.65-7.60 (2 H, m, ArH-3 or ArH-5, naphthyl-H), 7.58-7.56 (2 H, m, ArH-3 or ArH-5, naphthyl-H), 3.41 (3 H, s, CO_2CH_3); $^{13}\text{C-NMR}$ (100 MHz, CDCl_3): δ (ppm) 173.7 (C-5), 161.0 (CO_2CH_3), 158.9 (C-4), 136.4, 133.5, 132.9, 131.9, 131.8 (q, $J = 31.4$, ArC-6), 131.4, 130.9, 130.2, 129.4, 128.7, 127.6, 127.1 (ArC-1), 126.7, 124.9, 124.8, 124.2, 123.2 (q, $J = 274.4$, CF_3), 112.2 (C-4), 51.8 (CO_2CH_3), (not all peaks could be precisely assigned with certainty); LC-MS (ESI): calc. for $\text{C}_{22}\text{H}_{14}\text{ClF}_3\text{NO}_3$ $[\text{M}+\text{H}]^+$: 432.05, observed: 432.25, LC R_t : 8.14 min.

4.3.37. Methyl 5-{3-[(tert-butyldimethylsilyl)oxy]phenyl}-3-[2-chloro-6-(trifluoromethyl)phenyl]-1,2-oxazole-4-carboxylate (38). According to the General

Procedure for Suzuki coupling, bromide **30a** (0.400 g, 1.04 mmol) was coupled to 3-(4,4,5,5-Tetramethyl-1,3,2-dioxaborolan-2-yl)phenol (0.319 g, 1.45 mmol). The crude product was purified by flash column chromatography, eluting with a gradient of 10% - 20% EtOAc in n-heptane, to furnish the phenol (0.167 g, 40%) as a colourless solid.

Imidazole (94.0 mg, 1.38 mmol, 3.0 eq) and tert-butyldimethylsilyl chloride (0.104 g, 0.690 mmol, 1.5 eq) were added to a solution of the phenol (0.183 g, 0.460 mmol, 1.0 eq) in DMF (3.0 mL). The reaction mixture was stirred at room temperature for 3 h, then diluted with saturated aqueous NH_4Cl (20 mL) and extracted with EtOAc (2 x 20 mL). The combined organic phase was washed with water (2 x 50 mL) and brine (50 mL), dried (MgSO_4), filtered and concentrated in vacuo. The crude product was purified by column chromatography, eluting with a gradient of 0-20% EtOAc in n-heptane, to furnish silyl ether **38** (56.0 mg, 70%) as a colourless oil. R_f = 0.26 (9:1 n-heptane-EtOAc); $^1\text{H-NMR}$ (400 MHz, CDCl_3): δ (ppm) 7.73 (2 H, app. t, J = 8.6, ArH-3 and ArH-5), 7.70 (1 H, ddd, J = 8.1, 1.7, 1.0, phenol H-4), 7.59-7.55 (2 H, m, phenol H-2, ArH-4), 7.39 (1 H, app. t, J = 8.1, phenol H-5), 7.04 (1 H, ddd, J = 8.1, 2.4, 1.0, phenol H-6), 3.59 (3 H, s, CO_2CH_3), 1.02 (9 H, s, $\text{Si}(\text{CH}_3)_2\text{C}(\text{CH}_3)_3$), 0.26 (6 H, s, $\text{Si}(\text{CH}_3)_2\text{C}(\text{CH}_3)_3$); $^{13}\text{C-NMR}$ (100 MHz,

CDCl₃): δ (ppm) 172.7 (C-5), 161.4 (CO₂CH₃), 159.4 (C-3), 155.9 (phenol C-3), 136.4 (ArC-2), 132.9 (ArC-3), 131.7 (q, J = 31.3, ArC-6), 130.8 (ArC-4), 129.7 (phenol C-5), 127.6 (ArC-1), 127.5 (phenol C-1), 124.8 (q, J = 5.0, ArC-5), 123.7 (phenol C-6), 123.0 (q, J = 274.4, CF₃), 122.4 (phenol C-4), 120.8 (phenol C-2), 109.3 (C-4), 52.0 (CO₂CH₃), 25.8 (Si(CH₃)₂C(CH₃)₃), 18.3 (Si(CH₃)₂C(CH₃)₃), -4.3 (Si(CH₃)₂C(CH₃)₃); LC-MS (ESI): calc. for C₂₄H₂₆ClF₃NO₄Si [M+H]⁺: 512.12, observed: 512.25, LC R_t: 9.62 min.

4.3.38. 3-[2-Chloro-6-(trifluoromethyl)phenyl]-5-(furan-2-yl)-1,2-oxazole-4-carbaldehyde (39). Ester **34** (0.192 g, 0.516 mmol) was treated according to the General Procedure for conversion of esters to aldehydes, to furnish aldehyde **39** (0.169 g, 96%) as a colourless oil. The crude product was used without further purification. R_f = 0.51 (3:2 n-heptane-EtOAc); ¹H-NMR (400 MHz, CDCl₃): δ (ppm) 10.20 (1 H, s, CHO), 7.77 (1 H, dd, J = 1.8, 0.8, furanyl H-5), 7.76 (1 H, d, J = 8.0, Ar H-3 or ArH-5), 7.73 (1 H, d, J = 7.8, ArH-3 or ArH-5), 7.60 (1 H, app. t, J = 8.0, ArH-4), 7.55 (1 H, dd, J = 3.6, 0.8, furanyl H-3), 6.72 (1 H, dd, J = 3.6, 1.8, furanyl H-4); ¹³C-NMR (100 MHz, CDCl₃): δ (ppm) 182.8 (CHO), 164.1 (C-5), 154.7 (C-3), 147.2 (furanyl C-3), 142.2 (furanyl C-2), 136.2 (ArC-2), 133.1 (ArC-3), 131.8 (q, J = 31.5, ArC-6), 131.3 (ArC-4), 125.6 (ArC-1), 125.0 (q, J = 5.0,

ArC-5), 122.9 (q, $J = 274.5$, CF_3), 116.9 (furan C-5), 115.2 (C-4), 112.9 (furan C-4);

LC-MS (ESI): calc. for $\text{C}_{15}\text{H}_8\text{ClF}_3\text{NO}_3$ $[\text{M}+\text{H}]^+$: 342.01, observed: 342.08, LC R_t : 6.93 min.

4.3.39. 3-[2-Chloro-6-(trifluoromethyl)phenyl]-5-(thiophen-2-yl)-1,2-oxazole-4-carbaldehyde (40). Ester **35** (0.082 g, 0.210 mmol) was treated according to the General Procedure for conversion of esters to aldehydes. The crude product was purified by flash column chromatography, eluting with a gradient of 2% - 10% EtOAc in n-heptane, to furnish aldehyde **40** (0.048 g, 64%) as a colourless solid. $R_f = 0.28$ (4:1 n-heptane-EtOAc); $^1\text{H-NMR}$ (400 MHz, CDCl_3): δ (ppm) 9.78 (1 H, s, CHO), 8.32 (1 H, dd, $J = 3.9, 1.2$, thiophenyl H-5), 7.80-7.75 (3 H, m, ArH-3, ArH-5, thiophenyl H-3), 7.64 (1 H, app. t, $J = 8.1$, ArH-4), 7.29 (1 H, dd, $J = 5.1, 3.9$, thiophenyl H-4); $^{13}\text{C-NMR}$ (100 MHz, CDCl_3): δ (ppm) 182.2 (CHO), 168.0 (C-5), 159.0 (C-3), 136.6 (ArC-2), 133.4 (thiophenyl C-5), 132.9 (ArC-3), 132.8 (ArC-4), 132.3 (q, $J = 31.5$, ArC-6), 131.6 (thiophenyl C-3), 128.7 thiophenyl C-4), 127.0 (thiophenyl C-2), 125.3 (ArC-1), 125.2 (q, $J = 5.0$, ArC-5), 122.9 (q, $J = 274.5$, CF_3), 114.4 (C-4); LC-MS (ESI): calc. for $\text{C}_{15}\text{H}_8\text{ClF}_3\text{NO}_2\text{S}$ $[\text{M}+\text{H}]^+$: 357.98, observed: 358.17, LC R_t : 7.27 min.

4.3.40. 3-[2-Chloro-6-(trifluoromethyl)phenyl]-5-(1H-pyrrol-3-yl)-1,2-oxazole-4-carbaldehyde (**41**). Ester **36** (0.228 g, 0.486 mmol) was treated according to the General Procedure for conversion of esters to aldehydes with a modification: The reduction step was performed with 3.0 equivalents of reducing agent and without cooling; this step occurred with concomitant loss of the Boc protecting group. The crude product was purified by flash column chromatography, eluting with 30% EtOAc in n-heptane, to furnish aldehyde **41** (0.084 g, 51%) as a brown solid. R_f = 0.20 (7:3 n-heptane-EtOAc); $^1\text{H-NMR}$ (400 MHz, CDCl_3): δ (ppm) 9.62 (1 H, s, CHO), 8.77 (1 H, br. s, NH), 8.26 (1 H, app. dt, J = 3.3, 1.7, pyrrole H-2), 7.78 (1 H, d, J = 8.0, ArH-3 or ArH-5), 7.75 (1 H, d, J = 8.0, ArH-3 or ArH-5), 7.61 (1 H, app. t, J = 8.0, ArH-4), 7.02-6.95 (1 H, m, pyrrole H-5), 6.95 (1 H, dd, J = 2.7, 1.7, pyrrole H-4); $^{13}\text{C-NMR}$ (100 MHz, CDCl_3): δ (ppm) 182.8 (CHO), 170.7 (C-5), 160.0 (C-3), 133.6 (ArC-2), 133.3 (ArC-3), 132.3 (q, J = 31.5, ArC-6), 131.4 (ArC-4), 125.7 (ArC-1), 125.1 (q, J = 5.0, ArC-5), 123.8 (pyrrole C-2), 122.9 (q, J = 274.5, CF_3), 120.3 (pyrrole C-5), 113.2 (pyrrole C-3), 110.7 (C-4), 108.6 (pyrrole C-4); LC-MS (ESI): calc. for $\text{C}_{15}\text{H}_9\text{ClF}_3\text{N}_2\text{O}_2$ $[\text{M}+\text{H}]^+$: 341.02, observed: 341.08, LC R_t : 6.33 min.

1
2
3
4 **4.3.41. 3-[2-Chloro-6-(trifluoromethyl)phenyl]-5-(naphthalen-1-yl)-1,2-oxazole-4-**
5
6
7 **carbaldehyde (42).** Ester **37** (0.068 g, 0.160 mmol) was treated according to the General
8
9
10 Procedure for conversion of esters to aldehydes. The crude product was purified by flash
11
12
13 column chromatography, eluting with 17% EtOAc in n-heptane, to furnish aldehyde **42**
14
15
16 (0.039 g, 61%) as a colourless solid. R_f = 0.28 (4:1 n-heptane-EtOAc); $^1\text{H-NMR}$ (400 MHz,
17
18 CDCl_3): δ (ppm) 9.73 (1 H, s, CHO), 8.14 (1 H, d, J = 8.5, naphthyl-H), 8.02-7.98 (2 H, m,
19
20 naphthyl-H), 7.83 (1 H, dd, J = 7.1, 1.2, naphthyl-H), 7.79 (1 H, d, J = 8.0, ArH-3 or ArH-
21
22 5), 7.76 (1 H, d, J = 8.0, ArH-3 or ArH-5), 7.68-7.61 (4 H, m, ArH-4 and naphthyl-H); $^{13}\text{C-}$
23
24 NMR (100 MHz, CDCl_3): δ (ppm) 183.1 (CHO), 176.6 (C-5), 157.4 (C-4), 136.3, 133.8,
25
26 133.1, 132.9, 131.8 (q, J = 31.5, ArC-6), 131.4, 131.2, 130.1, 128.9, 128.5, 127.3, 126.1
27
28 (ArC-1), 125.1, 125.0 (q, J = 5.0, ArC-5), 124.7, 123.1 (q, J = 274.4, CF_3), 122.5, 118.7
29
30 (C-4), (not all peaks could be precisely assigned with certainty); LC-MS (ESI): calc. for
31
32 $\text{C}_{21}\text{H}_{12}\text{ClF}_3\text{NO}_2$ $[\text{M}+\text{H}]^+$: 402.04, observed: 401.92, LC R_t : 8.15 min.
33
34
35
36
37
38
39
40
41
42
43
44
45
46
47
48

49 **4.3.42. 5-{3-[(tert-Butyldimethylsilyl)oxy]phenyl}-3-[2-chloro-6-(trifluoromethyl)phenyl]-**
50
51
52 **1,2-oxazole-4-carbaldehyde (43).** Ester **38** (0.173 g, 0.340 mmol) was treated according
53
54
55 to the General Procedure for conversion of esters to aldehydes. The crude product was
56
57
58
59
60

purified by flash column chromatography, eluting with a gradient of 0-10% EtOAc in n-heptane, to furnish aldehyde **43** (0.123 g, 80%) as a colourless solid. R_f = 0.34 (9:1 n-heptane-EtOAc); $^1\text{H-NMR}$ (400 MHz, CDCl_3): δ (ppm) 9.94 (1 H, s, CHO), 7.77 (1 H, d, J = 8.0, ArH-3 or ArH-5), 7.74 (1 H, d, J = 8.0, ArH-3 or ArH-5), 7.63-7.59 (2 H, m, phenol H-4 and phenol H-5), 7.51 (1 H, app. t, J = 2.0, phenol H-2), 7.46 (1 H, app. t, J = 8.0, ArH-4), 7.11 (1 H, ddd, J = 8.2, 2.0, 1.0, phenol H-6), 1.02 (9 H, s, $\text{Si}(\text{CH}_3)_2\text{C}(\text{CH}_3)_3$), 0.27 (6 H, s, $\text{Si}(\text{CH}_3)_2\text{C}(\text{CH}_3)_3$); $^{13}\text{C-NMR}$ (100 MHz, CDCl_3): δ (ppm) 182.8 (CHO), 174.4 (C-5), 158.5 (C-3), 156.6 (phenol C-3), 136.4 (ArC-2), 133.2 (ArC-3), 132.0 (q, J = 31.6, ArC-6), 131.3 (ArC-4), 130.6 (phenol C-5), 126.8 (ArC-1), 126.0 (phenol C-1), 125.0 (q, J = 5.1, ArC-5), 124.6 (phenol C-6), 123.0 (q, J = 274.5, CF_3), 122.0 (phenol C-4), 120.3 (phenol C-2), 116.3 (C-4), 25.6 ($\text{Si}(\text{CH}_3)_2\text{C}(\text{CH}_3)_3$), 18.4 ($\text{Si}(\text{CH}_3)_2\text{C}(\text{CH}_3)_3$), -4.2 ($\text{Si}(\text{CH}_3)_2\text{C}(\text{CH}_3)_3$); LC-MS (ESI): calc. for $\text{C}_{23}\text{H}_{24}\text{ClF}_3\text{NO}_3\text{Si}$ $[\text{M}+\text{H}]^+$: 482.11, observed: 482.17, LC R_t : 9.45 min.

4.4. Biophysical Assays.

4.4.1. RORyt-LBD Expression and Purification (used for TR-FRET assays). A pET15b expression vector encoding the human RORyt LBD (residues 265-518) with an *N*-terminal

His₆-tag was transformed by heat shock into BL21(DE3) *E. coli* cells. Single colonies were used to inoculate pre-cultures of 8 mL LB-media containing 100 µg/mL ampicillin. After over-night incubation at 37 °C each pre-culture was transferred to 1L TB media supplemented with ampicillin (100 µg/mL) and incubated at 37 °C until an OD_{600 nm} = 1.0 was reached. Protein expression was then induced with 0.5 mM isopropyl-b-d-thiogalactoside (IPTG) and cultures were incubated for 16 h at 18°C. The cells were collected by centrifugation and suspended in lysis buffer (300 mM NaCl, 20 mM TrisHCl pH 8.0, 20 mM imidazole, 1 mM TCEP, 10% v/v glycerol, cOmplete™, EDTA-free Protease Inhibitor Cocktail tablets (1 tablet/ 50 mL lysate) and benzonase (0.1 µL/ 1 mL)). After lysis using a C3 Emulsiflex-C3 homogeniser (Avestin) the cell lysate was cleared by centrifugation at 4 °C and the protein was purified via Ni²⁺ affinity column chromatography. Fractions containing the protein of interest were combined and dialysed against: 150 mM NaCl, 20 mM TrisHCl pH 8.0, 5 mM DTT and 10% v/v glycerol.

4.4.2. TR-FRET Coactivator Recruitment Assay. Assays were conducted using 100 nM N-terminal biotinylated SRC-1 box2 peptide (Biotin-N-PSSHSSLTARHKILHRLLQEGSPSD-CONH₂) and 20 nM His₆-RORYt-LBD or 100 nM

His₆-PPAR_γ-LBD in buffer containing 10 mM HEPES, 150 mM NaCl, 5 mM DTT, 0.1% BSA (w/v) and 0.1 mM CHAPS, pH 7.5. A terbium labelled anti-His antibody (CisBio Bioassays, 61HISTLA) and D2-labelled streptavidin (CisBio Bioassays, 610SADLA) were used at the concentrations recommended by the supplier. In case of PPAR_γ, the assay was performed in the presence of 1 μM rosiglitazone, in order to initially activate PPAR_γ. Compounds (dissolved in DMSO) were titrated using a 2 x dilution series in Corning white low volume, low binding, 384-well plates at a final volume of 10 μL. The final DMSO concentration was 2% v/v throughout. The plate was incubated at room temperature for 30 min and centrifuged before reading (excitation = 340 nm; emission = 665 nm and 620 nm) on a Tecan infinite F500 plate reader using the parameters recommended by CisBio Bioassays. The data were analyzed with Origin Software. The dose-response curve was fitted represented by:

$$y = A_1 + \frac{A_2 - A_1}{1 + 10^{(\log(x_0) - x)p}}$$

Where y is the FRET ratio, A₁ is the bottom asymptote, A₂ is the top asymptote, p is the Hills slope and x is the ligand concentration. Where dose-response curves did not reach

a bottom asymptote this was fixed at the value of the negative control. (Data recorded in triplicate; error shown is standard deviation from the mean; curves are representative of > 3 repeated experiments).

4.4.3. Competition TR-FRET Coactivator Recruitment Assay. Competition assays were performed in an analogous fashion to that described above only in the presence of fixed concentrations of cholesterol: 0 μ M (DMSO), 0.25 μ M, 1.0 μ M such that the final concentration of DMSO remained at 1.2% v/v.

4.4.4. Ligand Binding TR-FRET Assay. Assays were conducted using 100 nM Alexa647-labelled MRL-871 and 20 nM His₆-RORYt-LBD in buffer as described above. A terbium-labelled anti-His antibody (CisBio Bioassays, 61HISTLA) was used at the concentrations recommended by the supplier. The assay was carried out in Corning black low volume, low binding, 384-well plates at a final volume of 10 μ L in the same manner as described above.

4.5. Protein X-Ray Crystallography.

4.5.1. ROR γ t-LBD Expression and Purification (used for crystallography).

A pET15b expression vector was ordered from GenScript encoding for the ROR γ t LBD (residues 265–507) containing a C455H mutation (ROR γ tC455H) and a C-terminal His-tag. The plasmid was transformed by heat shock into BL21(DE3) *E. coli* cells. A single colony was used to start three pre-cultures of 24 ml LB medium containing 100 μ g/ml ampicillin. After overnight incubation at 37 °C, each pre-culture was transferred to 2 liters of 2x YT medium supplied with 0.05 % antifoam SE-15 (Sigma-Aldrich). These cultures were incubated until they reached an OD₆₀₀=0.6. Protein expression was induced by adding 0.25 mM IPTG. The temperature was decreased to 15°C and protein expression proceeded overnight. The cells were collected by centrifugation at 10.000 RCF for 10 minutes at 4°C. The resulting 30 grams of cell pellet was dissolved in lysis buffer (20 mM Tris, 500 mM NaCl, 2 mM TCEP, 0.1% Tween20, 10% glycerol, 10 cOmplete™ Protease Inhibitor Cocktail tablets (Roche) and 25 U/ml Bezonase® Nuclease (Millipore), adjusted to pH=8.0). After cell lysis using an Emulsiflex-C3 homogeniser (Avestin), the cell lysate was cleared by centrifugation at 40.000 RCF for 40 minutes at 4°C and the supernatant was loaded on a 5 ml Ni-NTA Superflow cartridge (QIAGEN) pre-equilibrated with buffer A (20 mM Tris, 500 mM NaCl, 2 mM TCEP, 0.1% Tween20 and 10% glycerol). The column was washed with 10 CVs of buffer A supplied with 20 mM and sequentially with 10 CVs of Buffer A supplied with 50 mM imidazole. The protein was eluted from the resin using eight column volumes elution buffer (buffer A supplied with 200 mM imidazole). The purified protein was then dialysed overnight to buffer A containing 1.2 U of restriction-grade thrombin (Millipore) per milligram of purified protein to remove the His-tag. Next, the protein mixture was concentrated

using an Amicon® Ultra centrifugal filter with a 10-kDa cutoff (Millipore) and loaded on a Superdex 75 pg 16/60 size-exclusion column (GE Life Sciences) using 20 mM Tris, 100 mM NaCl and 5 mM DTT (adjusted to pH=8.0) as running buffer. The flow-through was collected as 3 ml fractions which were analyzed using Q-ToF LC/MS. The fractions containing ROR γ tC455H were combined and concentrated to a final concentration of 11.1 mg/ml. The concentrated protein sample was then aliquoted, flash-frozen and stored at -80°C.

4.5.2. X-Ray Crystallography.

The ROR γ tC455H solution (11.1 mg/ml) was mixed with 2 equivalents of **25** and incubated on ice for 1 hour. Next, the sample was centrifuged at 20,000 RCF for 20 minutes at 4°C to remove precipitated proteins. MRC-2 well crystallization plates (Hampton Research, sitting drop) were prepared using a Mosquito pipetting robot (TTP Labtech). Well-diffracting crystals were obtained by mixing 0.9 μ l of protein solution with 0.3 μ l of 1.6-2.0 M ammonium sulfate and 0.1 M Tris (pH=8.5). The well was filled with 80 μ l precipitant solution and plates were placed at 20°C. Crystals could be observed after one hour of incubation and grew to their final size overnight. The crystals were cryoprotected by transferring the crystals briefly to a solution containing 1.2M AmSO₄, 0.1 M Tris (pH=8.5) and 25% glycerol before being flash cooled in liquid N₂. Diffraction data were collected at 100 K at the P11 beamline of the PETRA III facility at DESY (Hamburg, Germany) and processed using the CCP4 suite (version 7.0.075).⁴⁷ DIALS was used to integrate and scale the data.⁴⁸ The data was phased with PHASER using 5C4O as a molecular replacement model and ligand restraints of **25** were generated with AceDRG.^{49,50} Sequential model building and refinement were performed with COOT and REFMAC respectively.^{51,52} PyMOL (version 2.2.3, Schrödinger) was used to make the figures.⁵³ The structure of ROR γ tC455 in complex with **25** was deposited in the protein data bank (PDB) under code 6SAL.

4.6. Quantitative IL-17a mRNA RT-PCR assay. EL4 cells (Sigma-Aldrich) were grown in DMEM (Gibco) with 10% FBS. At 24h after the cells were seeded onto a 12-well plate, the cells were incubated with 10 μ M compound (from 10 mM stock in DMSO) or DMSO for 24h, and activated with phorbol 12-myristate 13-acetate (PMA, 50 ng/mL; Sigma Aldrich) and ionomycin (1 μ g/mL; Sigma Aldrich) for 5h. The cells were then collected and RNA was isolated using a RNeasy Mini Kit (Qiagen) and reverse transcribed using the iScript Advanced cDNA Synthesis Kit (Bio-Rad). Quantitative RT-PCR was performed to analyze mRNA levels of mouse IL-17a levels (in triplicate) using SYBR green technology (Bio-Rad) on a CFX Real-Time System (Bio-Rad). The following primer assays were purchased from Bio-Rad: IL-17a (qMmuCID0026592) and Gapdh (qMmuCED0027497). The level of IL-17a mRNA expression was normalized to that of Gapdh expression. The relative gene expression was calculated by the $2^{-\Delta\Delta C_t}$ (Livak) method using the DMSO control as calibrator. (Data recorded in triplicate; error shown is standard deviation from the mean; data are representative of > 3 repeated experiments).

4.7. Absorption, Distribution, Metabolism and Excretion Experiments.

4.7.1 Chemical stability. Chemical stability was determined by incubating test compounds at a final concentration of 2 μ M in aqueous buffer at pH 7.4 for 1, 7 and 24h, respectively. The percentage of remaining compound (%remain) in relation to the zero time point was calculated following LCMS-based measurement of sample aliquots of each time point.

4.7.2 Kinetic solubility. Aqueous solubility of compounds was determined by spectrophotometrical measurement of the kinetic solubility of a 500 μ M compound solution in aqueous buffer pH 7.4 compared to a solution in the organic solvent acetonitrile after 90 minutes of vigorous shaking at room temperature.

4.7.3 PAMPA. Permeability through artificial membranes (PAMPA) was performed at an initial concentration of 500 μ M of the compound in the donor compartment. After an incubation period of 20 hours, absorption of the receiver wells was measured by spectrophotometry and permeation was calculated by normalization of the compound flux across a blank filter.

4.7.4 Microsomal stability phase I. Metabolic stability under oxidative conditions was measured in liver microsomes from different species by LCMS-based measuring of depletion of compound at a concentration of 3 μ M over time up to 50 minutes at 37°C. Based on compound half-life $t_{1/2}$, in vitro intrinsic clearance CL_{int} was calculated. $Cl_{int} = \frac{V \times 0.693}{t_{1/2} \times mg}$

4.7.5 Microsomal stability phase II. Metabolic stability under conjugative conditions was measured in the glucuronidation assay by LCMS-based determination of %remaining of selected compounds at a concentration of 5 μ M in incubations with liver microsomes supplemented with UDPGA for 1h at 37°C.

1
2
3 **4.7.6 Plasma Stability.** Plasma stability was measured by LCMS-based determination of
4
5 %remaining of selected compounds at a concentration of 5 μ M after incubation in 100% plasma
6
7 obtained from different species for 1h at 37°C.
8
9

10 **4.7.7. Plasma Protein Binding.** Assessment of plasma protein binding was measured by
11
12 equilibrium dialysis by incubating plasma with the compound of interest at a concentration of 5
13
14 μ M for 6h at 37°C followed by LC-MS-based determination of final compound concentrations.
15
16
17
18
19
20
21
22
23
24
25
26
27
28
29
30
31
32
33
34
35
36
37
38
39
40
41
42
43
44
45
46
47
48
49
50
51
52
53
54
55
56
57
58
59
60

ASSOCIATED CONTENT

Supporting information

CONTENTS

S1.0. *In silico* experiments.

Phase pharmacophore screen scores – Table S1 and S2.

Chem-T C-5 virtual library SMILES strings – Table S3.

Manually generated C-5 virtual library – Figure S1.

Glide docking scores – Table S4 and S5.

S2.0. Chemistry Supporting Information and Spectra.

S2.1. Regiochemical assignment of **30a**.

S2.2. Synthesis of **5** (Glenmark).

S2.3. NMR spectra and LC-UV traces for assayed compounds.

S3.0. Crystallography

Data collection and refinement statistics (molecular replacement) of **25** – Table S6.

Two-dimensional protein-ligand interaction plot for **25** – Figure S2.

Overlay of crystal structure and docking pose for **25** – Figure S3.

Molecular formula strings

Accession codes

Coordinates and structure factors for the ROR γ t bound to compound **25** have been deposited in the Protein Data Bank under accession code 6SAL. Authors will release the atomic coordinates and experimental data upon article publication.

AUTHOR INFORMATION

Corresponding Author

* E-mail: l.brunsveld@tue.nl

ORCID iD

Femke A. Meijer 0000-0003-4412-9968

Richard G. Doveston 0000-0002-7399-9607

Rens M.J.M. de Vries 0000-0002-1686-0027

Seppe Leysen 0000-0001-5567-1870

Marcel Scheepstra 0000-0001-6735-6528

Christian Ottmann 0000-0001-7315-0315

Lech-Gustav Milroy 0000-0003-4601-0936

Luc Brunsveld 0000-0001-5675-511X

Author Contributions

ξ FAM and RGD contributed equally to this work. The manuscript was written through contributions of all authors. RGD and SL performed *in silico* work; RGD, FAM, GMV and AAVV performed synthesis and biochemical studies; FAM performed RT-PCR experiments; RMJMV performed protein expression and crystallization studies; RGD, FAM, RMJMV, SL, MS, CO, LGM and LB designed the studies. All authors have given approval to the final version of the manuscript.

Funding Sources

This work was supported by the Netherlands Organization for Scientific Research through Gravity program 024.001.035, VICI grant 016.150.366, ECHO grant 711.018.003 and the European Union through a MSCA Individual Fellowship (R.G.D, H2020-MSCA-IEF-2016, grant number 705188).

Notes

The authors declare no competing financial interest.

ACKNOWLEDGMENT

We thank Rowin J.P.M. de Visser for synthesis of AlexaFluor647-labelled MRL-871 probe, Guido J.M. Oerlemans and Maxime C.M. van den Oetelaar for synthesis optimization, Iris A. Leijten - van de Gevel for expression of the RORyt protein (used for TR-FRET assays) and Joost L.J. van Dongen for performing HRMS measurements. We also thank the Lead Discovery Center in Dortmund (Matthias Baumann, Jan Eickhoff and Bert Klebl) for performing ADME measurements. Finally, we thank the DLS-CCP4 Data Collection and Structure Solution Workshop 2017 at Diamond Light Source (Oxfordshire, UK).

ABBREVIATIONS

AR, Androgen Receptor; DME, 1,2-Dimethoxyethane; DMF, Dimethylformamide; DMP, Dess-Martin periodinane; DPPA, diphosphoryl azide; H12, helix 12; IPTG, isopropyl- β -D-thiogalactoside; mAb, monoclonal antibody; NBS, *N*-bromosuccinimide; NCS, *N*-Chlorosuccinimide; NR, Nuclear Receptor; Q-tof, quadrupole time of flight; RORyt,

retinoic acid receptor-related orphan receptor γ t; RT-PCR, real time PCR; TFA, Trifluoroacetic acid; Th17, T helper 17; THF, Tetrahydrofuran; TR-FRET, time-resolved FRET.

REFERENCES

- (1) Wang, J.; Zou, J. X.; Xue, X.; Cai, D.; Zhang, Y.; Duan, Z.; Xiang, Q.; Yang, J. C.; Louie, M. C.; Borowsky, A. D.; Gao, A.; Evans, C. P.; Lam, K. S.; Xu, J.; Kung, H.-J.; Evans, R. M.; Xu, Yong; Chen, H.-W. ROR- γ drives androgen receptor expression and represents a therapeutic target in castration-resistant prostate cancer. *Nat. Med.* **2016**, *22*, 488-496.
- (2) Zhang, Y.; Wu, X.; Xue, X.; Li, C.; Wang, J.; Wang, R.; Zhang, C.; Wang, C.; Shi, Y.; Zou, L.; Li, Q.; Huang, Z.; Hao, X.; Loomes, K.; Wu D.; Chen, H.-W.; Xu, J.; Xu, Y. Discovery and characterization of XY101, a potent, selective, and orally bioavailable

ROR γ inverse agonist for treatment of castration-resistant prostate cancer. *J. Med. Chem.*

2019, *62*, 4716–4730.

(3) Ivanov, I. I.; McKenzie, B. S.; Zhou, L.; Tadokoro C. E.; Lepelley, A.; Lafaille, J.

J.; Cua, D. J.; Littman, D. R. The orphan nuclear receptor ROR γ t directs the differentiation

program of proinflammatory IL-17+ T helper cells. *Cell* **2006**, *126*, 1121–1133.

(4) Manel, N.; Unutmaz, D.; Littman, D. R. The differentiation of human TH-17 cells

requires transforming growth factor- β and induction of the nuclear receptor ROR γ t. *Nat.*

Immunol. **2008**, *9*, 641–649.

(5) Yang, X. O.; Pappu, B. P.; Nurieva, R.; Akimzhanov, A.; Kang, H. S.; Chung, Y.; Ma,

L.; Shah, B.; Panopoulos, A. D.; Schluns, K. S.; Watowich, S. S.; Tian, Q.; Jetten, A.

M.; Dong, C. T helper 17 lineage differentiation is programmed by orphan nuclear

receptors ROR α and ROR γ . *Immunity* **2008**, *28*, 29–39.

(6) Miossec, P.; Kolls, J. K. Targeting IL-17 and TH17 cells in chronic inflammation. *Nat.*

Rev. Drug Discov. **2012**, *11*, 763–776.

(7) Burkett, P. R.; Kuchroo, V. K. IL-17 blockade in psoriasis. *Cell* **2016**, *167*, 1669.

(8) Lock, C.; Hermans, G.; Pedotti, R.; Brendolan, A.; Schadt, E.; Garren, H.; Langer-Gould, A.; Strober, S.; Cannella, B.; Allard, J.; Klonowski, P.; Austin, A.; Lad, N.; Kaminski, N.; Galli, S. J.; Oksenberg, J. R.; Raine, C. S.; Heller, R.; Steinman, L. Gene-microarray analysis of multiple sclerosis lesions yields new targets validated in autoimmune encephalomyelitis. *Nat. Med.* **2002**, *8*, 500–508.

(9) Duerr, R. H.; Taylor, K. D.; Brant, S. R.; Rioux, J. D.; Silverberg, M. S.; Daly, M. J.; Steinhardt, A. H.; Abraham, C.; Regueiro, M.; Griffiths, A.; Dassopoulos, T.; Bitton, A.; Yang, H.; Targan, S.; Datta, L. W.; Kistner, E. O.; Schumm, L. P.; Lee, A. T.; Gregersen, P. K.; Barmada, M. M.; Rotter, J. I.; Nicolae, D. L.; Cho, J. H. A genome-wide association study identifies IL23R as an inflammatory bowel disease gene. *Science*, **2006**, *314*, 1461–3.

(10) Hueber, W.; Patel, D. D.; Dryja, T.; Wright, A. M.; Koroleva, I.; Bruin, G.; Antoni, C.; Draelos, Z.; Gold, M. H.; Psoriasis Study Group; Durez, P.; Tak, P. P.; Gomez-Reino, J. J.; Rheumatoid Arthritis Study Group; Foster, C. S.; Kim, R. Y.; Samson, C. M.; Falk, N. S.; Chu, D. S.; Callanan, D.; Nguyen, Q. D.; Uveitis Study Group; Rose, K.; Haider,

A.; Di Padova, F. Effects of AIN457, a fully human antibody to interleukin-17A, on psoriasis, rheumatoid arthritis, and uveitis. *Sci. Transl. Med.* **2010**, *2*, 52-72.

(11) Attia, A.; Abushouk, A. I.; Ahmed, H.; Gadelkarim, M.; Elgebaly, A.; Hassan, Z.; Abdel-Daim, M. M.; Negida, A. Safety and efficacy of brodalumab for moderate-to-severe plaque psoriasis: A systematic review and meta-analysis. *Clin. Drug Investig.* **2017**, *37*, 439–451.

(12) Mease, P. J.; van der Heijde, D.; Ritchlin, C. T.; Okada, M.; Cuchacovich, R. S.; Shuler, C. L.; Lin, C. Y.; Braun, D. K.; Lee, C. H.; Gladman, D. D.; SPIRIT-P1 Study Group. Ixekizumab, an interleukin-17A specific monoclonal antibody, for the treatment of biologic-naïve patients with active psoriatic arthritis: results from the 24-week randomised, double-blind, placebo-controlled and active (adalimumab)-controlled period of the phase III trial SPIRIT-P1. *Ann. Rheum. Dis.* **2017**, *76*, 79–87.

(13) Fauber, B. P.; Magnuson, S. Modulators of the nuclear receptor retinoic acid receptor-related orphan receptor- γ (ROR γ or ROR γ c). *J. Med. Chem.* **2014**, *57*, 5871–92.

(14) Bronner, S. M.; Zbieg, J. R.; Crawford, J. J. ROR γ antagonists and inverse agonists: a patent review. *Expert Opin. Ther. Pat.* **2017**, *27*, 101–112.

- (15) Pandya, V. B.; Kumar, S.; Sachchidanand; Sharma, R.; Desai, R. C. Combating autoimmune diseases with retinoic acid receptor-related orphan receptor- γ (ROR γ or ROR γ c) inhibitors: hits and misses. *J. Med. Chem.* **2018**, *61*, 10976-10995.
- (16) Tanis, V. M.; Venkatesan, H.; Cummings, M. D.; Albers, M.; Kent Barbay, J.; Herman, K.; Kummer, D. A.; Milligan, C.; Nelen, M. I.; Nishimura, R.; Schlueter, T.; Scott, B.; Spurlino, J.; Wolin, R.; Woods, C.; Xue, X.; Edwards, J. P.; Fourie, A. M.; Leonard, K. 3-Substituted quinolines as ROR γ t inverse agonists. *Bioorg. Med. Chem. Lett.* **2019**, *29*, 1463-1470.
- (17) Imura, C.; Ueyama, A.; Sasaki, Y.; Shimizu, M.; Furue, Y.; Tai, N.; Tsujii, K.; Katayama, K.; Okuno, T.; Shichijo, M.; Yasui, K.; Yamamoto, M. A novel ROR γ t inhibitor is a potential therapeutic agent for the topical treatment of psoriasis with low risk of thymic aberrations *J. Dermatol. Sci.* **2019**, *93*, 176-185.
- (18) Tian, J.; Sun, N.; Yu, M.; Gu, X.; Xie, Q.; Shao, L.; Liu, J.; Liu, L.; Wang, Y. Discovery of *N*-indanyl benzamides as potent ROR γ t inverse agonists. *Eur. J. Med. Chem.* **2019**, *167*, 37-48.

(19) Kotoku, M.; Maeba, T.; Fujioka, S.; Yokota, M.; Seki, N.; Ito, K.; Suwa, Y.; Ikenogami, T.; Hirata, K.; Hase, Y.; Katsuda, Y.; Miyagawa, N.; Arita, K.; Asahina, K.; Noguchi, M.; Nomura, A.; Doi, S.; Adachi, T.; Crowe, P.; Tao, H.; Thacher, S.; Hashimoto, H.; Suzuki, T.; Shiozaki, M. Discovery of second generation ROR γ inhibitors composed of an azole scaffold. *J. Med. Chem.* **2019**, *62*, 2837-2842.

(20) Duan, J. J.; Lu, Z.; Jiang, B.; Stachura, S.; Weigelt, C. A.; Sack, J. S.; Khan, J.; Ruzanov, M.; Galella, M. A.; Wu, D. R.; Yarde, M.; Shen, D. R.; Shuster, D. J.; Borowski, V.; Xie, J. H.; Zhang, L.; Vanteru, S.; Gupta, A. K.; Mathur, A.; Zhao, Q.; Foster, W.; Salter-Cid, L. M.; Carter, P. H.; Dhar, T. G. M. Structure-based discovery of phenyl (3-phenylpyrrolidin-3-yl)sulfones as selective, orally active ROR γ t inverse agonists. *ACS Med. Chem. Lett.* **2019**, *10*, 367-373.

(21) Gronemeyer, H.; Gustafsson, J.-Å.; Laudet, V. Principles for modulation of the nuclear receptor superfamily. *Nat. Rev. Drug Discov.* **2004**, *3*, 950–964.

(22) Li, X.; Anderson, M.; Delphine, C.; Muegge, I.; Wan, J.; Brennan, D.; Kugler, S.; Terenzio, D.; Kennedy, C.; Lin, S.; Labadia, M. E.; Cook, B.; Hughes, R.; Farrow, N. A. Structural studies unravel the active conformation of apo ROR γ t nuclear receptor and a

common inverse agonism of two diverse classes of ROR γ t inhibitors. *J. Biol. Chem.* **2017**, *292*, 11618-11630.

(23) Harris, J. M.; Lau, P.; Chen, S. L.; Muscat, G. E. O. Characterization of the retinoid orphan-related receptor- α coactivator binding interface: a structural basis for ligand-independent transcription. *Mol. Endocrinol.* **2002**, *16*, 998–1012.

(24) Hu X.; Wang, Y.; Hao, L. Y.; Liu, X.; Lesch, C. A.; Sanchez, B. M.; Wendling, J. M.; Morgan, R. W.; Aicher, T. D.; Carter, L. L.; Toogood, P. L.; Glick, G. D. Sterol metabolism controls TH17 differentiation by generating endogenous ROR γ agonists. *Nat. Chem. Biol.* **2015**, *11*, 141–147.

(25) Huh, J. R.; Leung, M. W.; Huang, P.; Ryan, D. A.; Krout, M. R.; Malapaka, R. R.; Chow, J.; Manel, N; Ciofani, M.; Kim, S. V.; Cuesta, A.; Santori, F. R.; Lafaille, J. J.; Xu, H. E.; Gin, D. Y.; Rastinejad, F.; Littman, D. R. Digoxin and its derivatives suppress TH17 cell differentiation by antagonizing ROR γ t activity. *Nature* **2011**, *472*, 486–490.

- (26) Kumar, N.; Solt, L. A.; Conkright, J. J.; Wang, Y.; Istrate, M. A.; Busby, S. A. Garcia-Ordonez, R. D.; Burris, T. P.; Griffin, P. R.; The benzenesulfoamide T0901317 [N-(2,2,2-trifluoroethyl)-N-[4-[2,2,2-trifluoro-1-hydroxy-1-(trifluoromethyl)ethyl]phenyl]-benzenesulfonamide] is a novel retinoic acid receptor-related orphan receptor-alpha/gamma inverse agonist. *Mol. Pharmacol.* **2010**, *77*, 228-236.
- (27) Overington, J. P.; Al-Lazikani, B.; Hopkins, A. L. How many drug targets are there? *Nat. Rev. Drug Discov.* **2006**, *5*, 993–996.
- (28) Meijer, F. A.; Leijten-van de Gevel, I. A.; de Vries, R. M. J. M.; Brunsveld, L. Allosteric small molecule modulators of nuclear receptors. *Mol. Cell Endocrinol.* **2019**, *485*, 20-34.
- (29) Tice, C. M.; Zheng, Y.-J. Non-canonical modulators of nuclear receptors. *Bioorg. Med. Chem. Lett.* **2016**, *26*, 4157-4164.
- (30) Moore, T. W.; Mayne, C. G.; Katzenellenbogen, J.; Not picking pockets: nuclear receptor alternate-site modulators (NRAMs). *Mol. Endocrinol.* **2010**, *24*, 683–95.
- (31) Scheepstra, M.; Leysen, S.; van Almen, G. C.; Miller, J. R.; Piesvaux, J.; Kutilek, V.; van Eenennaam, H.; Zhang, H.; Barr, K.; Nagpal, S.; Soisson, S. M.; Kornienko, M.; Wiley, K.; Elsen, N.; Sharma, S.; Correll, C. C.; Trotter, B. W.; van der Stelt,

M.; Oubrie, A.; Ottmann, C.; Parthasarathy, G.; Brunsveld, L. Identification of an allosteric binding site for ROR γ t inhibition. *Nat. Commun.* **2015**, *6*, 8833.

(32) Ouvry, G.; Bouix-Peter, C.; Ciesielski, F.; Chantalat, L.; Christin, O.; Comino, C.; Duvert, D.; Feret, C.; Harris, C. S.; Lamy, L.; Luzy, A. P.; Musicki, B.; Orfila, D.; Pascau, J.; Parnet, V.; Perrin, A.; Pierre, R.; Polge, G.; Raffin, C.; Rival, Y.; Taquet, N.; Thoreau, E.; Hennequin, L. F. Discovery of phenoxyindazoles and phenylthioindazoles as ROR γ inverse agonists. *Bioorg. Med. Chem. Lett.* **2016**, *26*, 5802–5808.

(33) Guo, Y.; MacIsaac, K. D.; Chen, Y.; Miller, R. J.; Jain, R.; Joyce-Shaikh, B.; Ferguson, H.; Wang, I. M.; Cristescu, R.; Mudgett, J.; Engstrom, L.; Piers, K. J.; Baltus, G. A.; Barr, K.; Zhang, H.; Mehmet, H.; Hegde, L. G.; Hu, X.; Carter, L. L.; Aicher, T. D.; Glick, G.; Zaller, D.; Hawwari, A.; Correll, C. C.; Jones, D. C.; Cua, D. J. Inhibition of ROR γ T skews TCR α gene rearrangement and limits T cell repertoire diversity. *Cell Rep.* **2016**, *17*, 3206–3218.

(34) Zhong, C.; Zhu, J. Small-molecule ROR γ t antagonists: one stone kills two birds. *Trends Immunol.* **2017**, *38*, 229–231.

(35) Gege, C. Retinoid-related orphan receptor γ t modulators: comparison of Glenmark's me-too patent application (WO2015008234) with the originator application from Merck Sharp and Dohme (WO2012106995). *Expert Opin. Ther. Pat.* **2015**, *25*, 1215–1221.

(36) Dixon, S. L.; Smondyrev, A. M.; Knoll, E. H.; Rao, S. N.; Shaw, D. E.; Friesner, R. A. PHASE: A new engine for pharmacophore perception, 3D QSAR model development, and 3D database screening: 1. Methodology and preliminary results. *J. Comput. Aided. Mol. Des.* **2006**, *20*, 647–671.

(37) Dixon, S. L.; Smondyrev, A. M.; Rao, S. N. PHASE: A novel approach to pharmacophore modeling and 3D database searching. *Chem. Biol. Drug Des.* **2006**, *67*, 370–372.

(38) Asinex Corp. Gold and platinum collections, release: 1994-2004, update: 2016-10. www.asinex.com/libraries-html/libraries_gold_platinum-html.

(39) Kalin, J. H.; Zhang, H.; Gaudrel-Grosay, S.; Vistoli, G.; Kozikowski, A. P. Chiral mercaptoacetamides display enantioselective inhibition of histone deacetylase 6 and exhibit neuroprotection in cortical neuron models of oxidative stress. *ChemMedChem* **2012**, *7*, 425–39.

- (40) Friesner, R. A.; Banks, J. L.; Murphy, R. B.; Halgren, T. A.; Klicic, J. J.; Mainz, D. T.; Repasky, M. P.; Knoll, E. H.; Shelley, M.; Perry, J. K.; Shaw, D. E.; Francis, P.; Shenkin, P. S. Glide: A new approach for rapid, accurate docking and scoring. 1. method and assessment of docking accuracy. *J. Med. Chem.* **2004**, *47*, 1739–1749.
- (41) Halgren, T. A.; Murphy, R. B.; Friesner, R. A.; Beard, H. S.; Frye, L. L.; Pollard, W. T.; Banks, J. L. Glide: A new approach for rapid, accurate docking and scoring. 2. enrichment factors in database screening. *J. Med. Chem.* **2004**, *47*, 1750-1759.
- (42) Abreu, R. M. V.; Froufe, H. J. C.; Daniel, P. O. M.; Queiroz, M. J. R. P.; Ferreira, I. C. F. R. ChemT, an open-source software for building template-based chemical libraries. *SAR QSAR Environ. Res.* **2011**, *22*, 603–610.
- (43) Leroy, J. Preparation of 3-bromopropiolic esters: methyl and tert-butyl 3-bromopropiolates. *Org. Synth.* **1997**, *74*, 212.
- (44) Oakdale, J. S.; Sit, R. K.; Fokin, V. V.; Ruthenium-catalyzed cycloadditions of 1-haloalkynes with nitrile oxides and organic azides: synthesis of 4-haloisoxazoles and 5-halotriazoles. *Chem. Eur. J.* **2014**, *20*, 11101–11110.

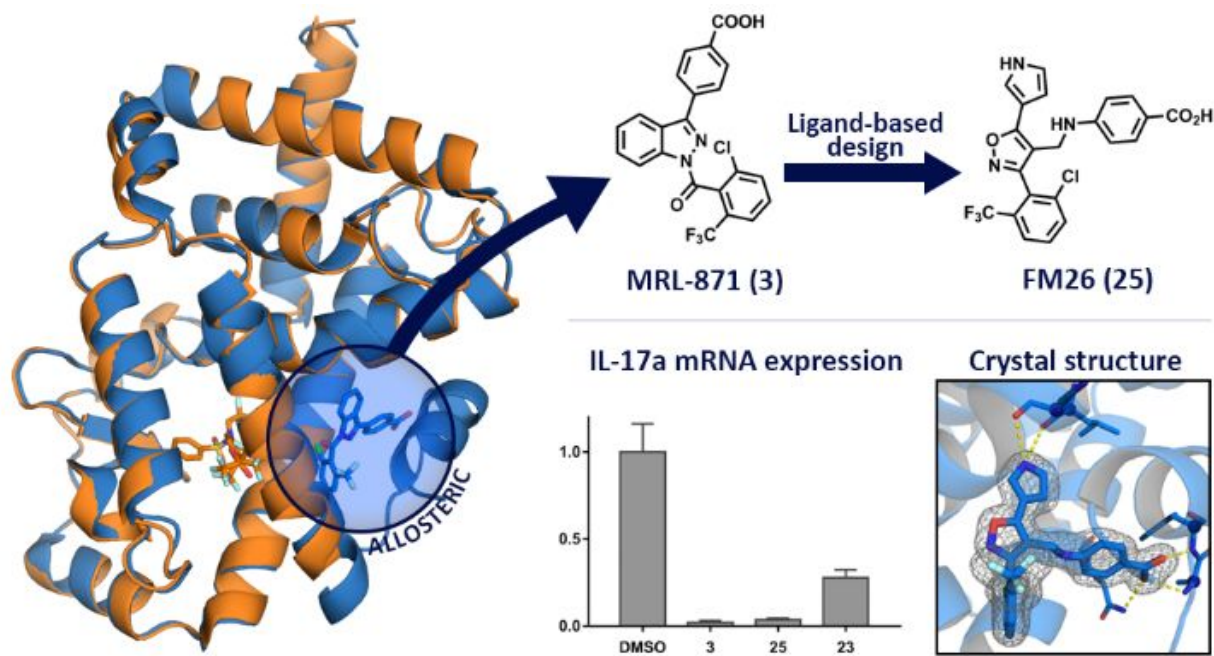
- (45) Buckman, D. O.; Nicholas, J. B.; Emayan, K.; Seiwert, S. D.; Yuan, S. Lysophosphatidic acid receptor antagonists. International patent WO/2014/113485, **2014**.
- (46) Potterton, L.; Agirre, J.; Ballard, C.; Cowtan, K.; Dodson, E.; Evans, P. R.; Jenkins, H. T.; Keegan, R.; Krissinel, E.; Stevenson, K.; Lebedev, A.; McNicholas, S. J.; Nicholls, R.A.; Noble, M.; Pannu, N.S.; Roth, C.; Sheldrick, G.; Skubak, P.; Turkenburg, J.; Uski, V.; von Delft, F.; Waterman D.; Wilson, K.; Winn, M.; Wojdyr, M. CCP412: the new graphical user interface to the CCP4 program suite. *Acta Crystallogr. D. Struct. Biol.* **2018**, *74*, 68-84.
- (47) Clabbers, M. T. B.; Gruene, T.; Parkhurst, J.M.; Abrahams, J.P.; Waterman, D.G. Electron diffraction data processing with DIALS. *Acta Crystallogr. D. Struct. Biol.* **2018**, *74*, 506-518.
- (48) McCoy, A. J. Solving structures of protein complexes by molecular replacement with Phaser. *Acta Crystallogr. D. Struct. Biol.* **2007**, *63*, 32-41.
- (49) Long, F.; Nicholls, R. A.; Emsley, P.; Grazulis, S; Merkys, A; Vaitkus, A.; Murshudov, G. N. *AceDRG*: a stereochemical description generator for ligands. *Acta Crystallogr. D. Struct. Biol.* **2017**, *73*, 112-122.

(50) Emsley, P.; Lohkamp, B.; Scott, W.G.; Cowtan, K. Features and development of Coot. *Acta Crystallogr. D. Struct. Biol.* **2010**, *66*, 486-501.

(51) Murshudov, G. N.; Skubák, P.; Lebedev, A. A.; Pannu, N. S.; Steiner, R. A.; Nicholls, R. A.; Winn, M. D.; Long, F.; Vagin, A. A. *REFMAC5* for the refinement of macromolecular crystal structures. *Acta Crystallogr. D. Struct. Biol.* **2011**, *67*, 355-367.

(52) The PyMOL Molecular Graphics System, Version 2.2.3 Schrödinger, LLC.

TABLE OF CONTENTS GRAPHIC



For Table of Contents Only.